Lateral Line Ablation by Toxins Results in Distinct Rheotaxis Profiles in Fish

Kyle C Newton[1]*, Dovi Kacev[2], Simon R O Nilsson[3], Sam A Golden[3], and Lavinia Sheets[1,4]*

[1] Department of Otolaryngology, Washington University School of Medicine, St. Louis, MO, USA

[2] Scripps Institution of Oceanography, University of California San Diego, La Jolla, CA, USA

[3] Department of Biological Structure, University of Washington, Seattle, WA, USA

[4] Department of Developmental Biology, Washington University School of Medicine, St. Louis, MO, USA

*** Correspondence:**

Kyle C Newton (kyle.newton@wustl.edu)

Lavinia Sheets (sheetsl@wustl.edu)

Keywords: zebrafish, lateral line, neuromast, sensory hair cell, rheotaxis, pose estimation, animal tracking, behavior classification, behavioral profile, machine learning, machine vision

ABSTRACT

Zebrafish lateral line is an established model for hair cell organ damage, yet few studies link mechanistic disruptions to changes in biologically relevant behavior. We used larval zebrafish to determine how damage via ototoxic chemicals impact rheotaxis. Larvae were treated with $CuSO_4$ or neomycin to disrupt lateral line function then exposed to water flow stimuli. Their swimming behavior was recorded, and DeepLabCut and SimBA software were used to track movements and classify rheotaxis behavior. Lateral line-disrupted fish performed rheotaxis, but they swam greater distances, for shorter durations, and with greater angular variance than controls. Further, spectral decomposition analyses demonstrated that lesioned fish exhibited toxin-specific behavioral profiles with distinct fluctuations in the magnitude, timing, and cross-correlation between changes in linear and angular movements. Our observations support that lateral-line input is needed for fish to perform rheotaxis efficiently in flow and reveals commonly used lesion methods have unique effects on behavior.

INTRODUCTION

The lateral line is a sensory system used by fishes and amphibians to detect water flow. The functional units of the lateral line are neuromasts; bundles of sensory hair cells located externally along the head and body that mechanotransduce low frequency (≤ 200 Hz) water flow stimuli into electrochemical signals for interpretation by the central nervous system (reviewed in [1]). The lateral line is known to partially mediate rheotaxis, a multimodal behavior ([2]) that integrates input from visual ([3], [4], [5]vestibular ([6], [7]), tactile ([3], [8], [9], [10]), and lateral line systems ([9], [10], [8]) to facilitate fish orientation and movement with respect to water flow ([9], [10]).

Although contribution from the lateral line is well established, there is conflicting evidence on whether it is essential for rheotaxis in fish ([2] , [5], [9], [10], [11], [12]). Inconsistent methodologies used on several species that differentially rely on the lateral line to mediate behavior obfuscate the relationship between the lateral line and rheotaxis. However, a recent

review hypothesized that differences in the spatial characteristics and velocity of the flow stimuli used to assay rheotaxis likely resulted in the disparate results reported in these studies (see Table 1 in [13]).

Zebrafish hair cells demonstrate unique regenerative features that make them an important model for hearing loss research ([14], [15], [16], [17], [18], [19]). Many studies have focused on mechanistic disruption of hair cell activity, but few have explored the association between this disruption and behavior. Previous researchers have developed several different assays to study rheotaxis in larval fishes (e.g. [5], [20], [21], [22]). However, we sought to develop a behavioral assay and analytical methodology that is sensitive, spatiotemporally scalable, and robust enough to be used on a variety of species, ontogenetic stages, sensory modalities, and behavioral responses that are pertinent to biomedical and ecological research.

We therefore investigated how the lateral line contributes to rheotaxis in larval zebrafish and developed a standardized assay that could identify previously observed subtle differences in rheotaxis behavior ([12]). We compared the rheotaxis response of fish with an intact lateral line to those with lateral lines ablated by two commonly used compounds: copper sulfate ($CuSO_4$; [17], [23], [24], [25]) and neomycin ([5], [15], [26]). We hypothesized that different toxins produce distinct changes in rheotaxis behavior because they injure lateral lines via different cellular mechanisms ([27]), and that these changes may be quantified objectively with machine vision and learning techniques.

RESULTS & DISCUSSION

To determine the contribution of the lateral line to rheotaxis in fishes we used $CuSO_4$ and neomycin to ablate the lateral line neuromasts of larval zebrafish (6-7 days post-fertilization (dpf)), then video recorded the swimming behavior of individual larvae in a microflume under no-flow and flow stimulus conditions (Fig. 1). Although it was not possible to selectively block tactile cues, young larval zebrafish are not known to detect horizontal angular velocity cues (i.e. yaw) and our procedures eliminated linear acceleration and visual cues (see methods). We used

machine vision and learning software to annotate videos for positive rheotaxis events where fish were oriented to 0° ± 45° and actively swam into the oncoming flow (Fig. 2). Under no flow conditions, we determined that each treatment group of fish was randomly distributed (Fig. 3; Supplementary Table 1) and had no natural proclivity to orient their bodies to 0° ± 45° (Supplementary Table S2). We standardized our analyses by comparing rheotaxis data acquired during flow to the swimming behavior of fish when they were randomly oriented at 0° ± 45° under no flow. A subset of all fish that had undergone behavioral testing were fixed and immunolabeled to confirm lateral line organ ablation (Supplementary Fig. 1).

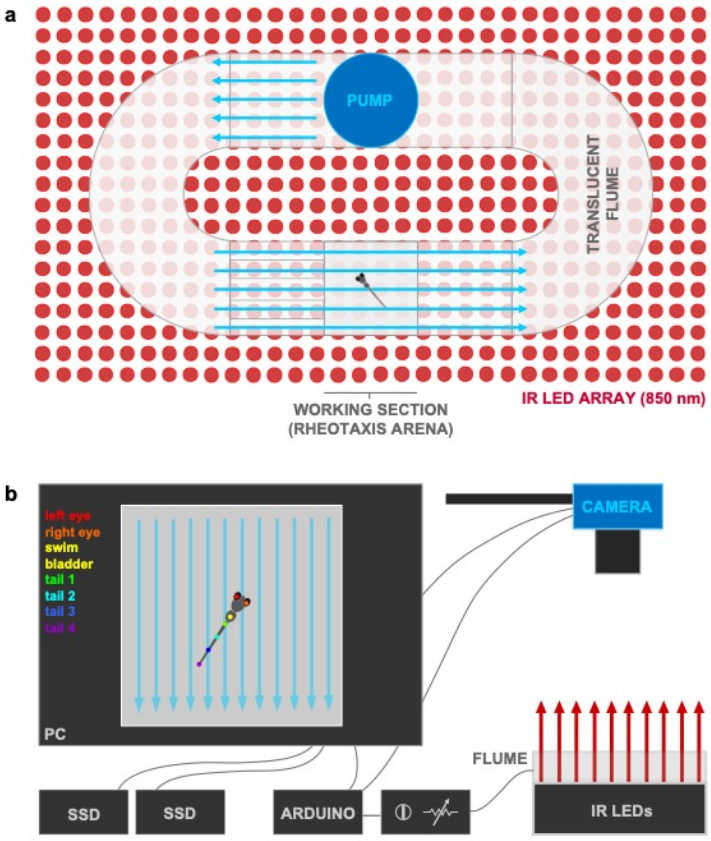

Figure 1. Experimental microflume used to conduct rheotaxis assays under IR illumination. a) The microflume (220 x 100 x 40 mm) with a removeable working section (30 x 30 x 10 mm) was 3D printed from translucent resin and placed on top of an infrared (850 nm) LED array. b) Schematic of experimental set-up. The IR light passed through the flume and the overhead camera recorded rheotaxis trials at either 200 or 60 fps onto SD cards. The timing and duration for the camera and flume pump onset and offset of was controlled by an Arduino and pump voltage (i.e. water flow velocity ~ 10 mm s^{-1}) was controlled by a rheostat. Each

trial was monitored via the live camera feed displayed on the PC and all videos were copied in duplicate onto a 10TB RAID array. Dots on fish larva indicate seven body positions tracked by DeepLabCut.

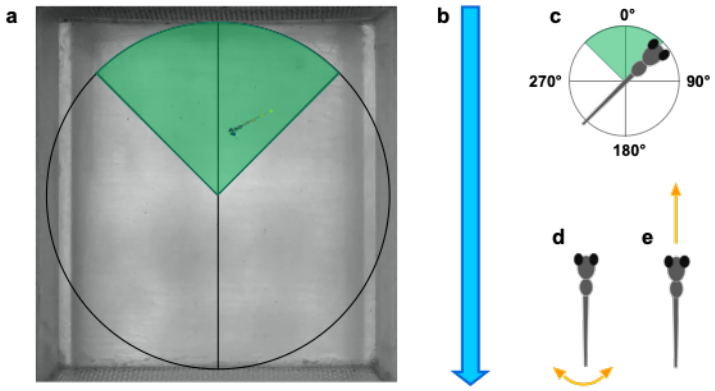

Figure 2. Definition of positive rheotaxis behavior. a) Larval zebrafish in the microflume arena performing rheotaxis under flow as defined by multiple conditions, including: b) the water flow stimulus was on; c) the fish body angle was oriented to 0° ± 45° (green shaded wedge); d) the tail moved laterally every 100 ms; and e) the body of the fish had forward translation every 100 ms. Note that conditions (d) and (e) were used to discriminate between fish displaying positive rheotaxis and those passively drifting backward with body angles of 0° ± 45°.

Lateral Line Ablation Alters but Does Not Eliminate Rheotaxis Behavior

We predicted that fish treated with the minimum dosage of $CuSO_4$ or neomycin necessary to completely ablate lateral line hair cells of the lateral line would not perform rheotaxis as well as control fish with an intact lateral line. Surprisingly, fish lacking intact lateral line organs could still orient into oncoming flow similar to control fish (Fig. 3; Supplementary Tables 1-2), indicating that the effects of lateral line ablation were subtle and not essential for rheotaxis behavior.

When analyzing individual components of rheotaxis, stark behavioral changes were observed among lesioned fish. Comparisons between lateral line-ablated and control groups showed significant differences in the mean body angle or angular variance (Fig. 3, Supplementary Table 3), mean duration of rheotaxis events, mean number of rheotaxis events, total distance traveled, and latency to the onset of rheotaxis (Fig. 4, Supplementary Tables 4-7).

These observations suggest that rheotaxis occurs but is altered in lateral line-ablated groups, contrasting with previous reports on larval zebrafish ([5], [22], [28]) and supporting the idea that the lateral line is not required for rheotaxis in fish ([2], [11], [12], [29], [30]). We believe that our focus on acute rheotaxis behavior and use of fine scale spatiotemporal sampling and machine vision allowed us to detect subtle changes in rheotaxis behavior that were overlooked in previous studies ([2], [5], [12], [29], [30]). Our methods eliminated water motion, optic flow ([3]), and certain vestibular cues (yaw: [31], [32]; linear acceleration: see methods). However, tactile cues were not eliminated because we could not prevent fish from contacting the substrate and our flow rate was sufficient to displace substrate coupled fish backward and against the rear mesh of arena. Therefore, we propose that lateral line ablated fish predominantly used tactile cues to gain an external frame of reference and perform rheotaxis ([8], [10]).

Toxins Differentially Influence the Distribution of Mean Body Angles During Flow

To identify differences in body orientation, the mean body angle for fish in the presence or absence of flow stimuli were compared among treatment groups (Fig. 3). Since flow originated at the top of the flume (located at 0°), mean body angle was determined relative to the oncoming water stimulus. Angular variance of each group is represented by the inverse of the mean resultant vector length (i.e. short vectors = high variance, and vice versa; Fig. 3). Under no flow, fish from each treatment group swam with a random orientation, indicated by a grand mean body angle that was statistically different from 0° and resultant vector length close to zero (Fig. 3a, Supplementary Table 2). When flow was applied, all groups exhibited a grand mean body angle clustered around 0° and resultant length close to one (Fig. 3b-c), thus demonstrating significant alignment into the oncoming flow stimulus.

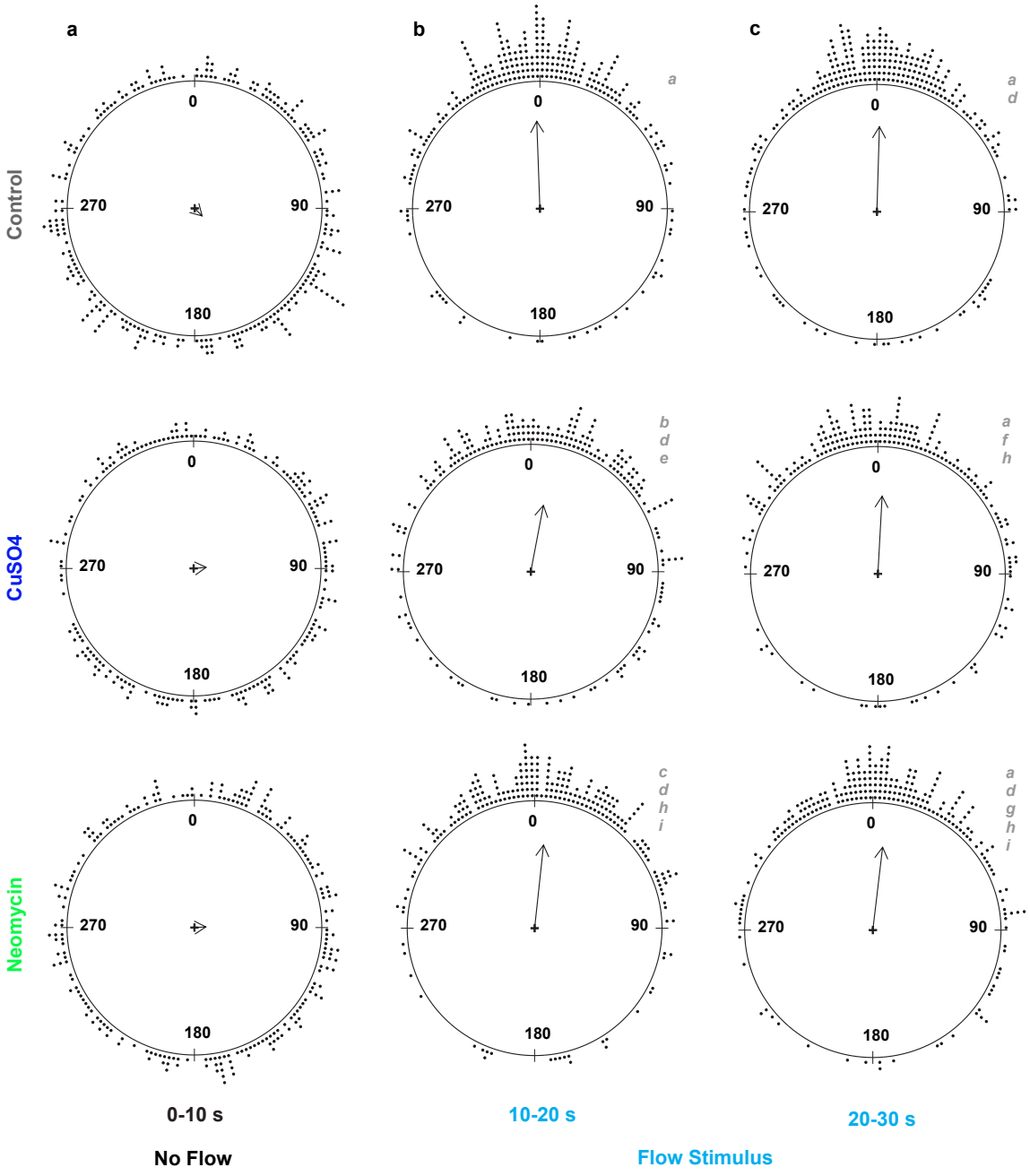

Figure 3. The mean resultant vectors of fish treatment groups before and during water flow stimulus indicates fish with lateral-line organs ablated by $CuSO_4$ or neomycin can still perform rheotaxis. Each dot outside the circles represents the mean body angle of an individual fish for the 10 s duration of the no flow and flow stimulus conditions. The grand mean vector for each group is represented by a summary vector with an angle, *theta*, and a mean resultant length, *rho*, where the length of the vector represents the distribution of individual angles around the mean angle of the group. The length of the vector ranges from zero for uniform distributions, to one for distributions perfectly aligned with the mean angle. Consequently, the angular variance (1- *rho*) is inversely related to vector length. Under no flow (t = 0-10 s), groups of lateral line intact (control) and lesioned (CuSO4, neomycin)

fish have a random distribution of individual mean body angles. Under flow, all groups show a statistically significant orientation to 0° ± 45°, but the distributions of the individual mean angles within the groups differ between the initial (t = 10-20 s) and final (t = 20-30 s) stimulus bins. Distributions with the same lowercase letter indicate groups that do not differ statistically.

During rheotaxis, post-hoc comparisons within treatment groups showed a significant difference in the homogeneity of distributions between initial and final portions of the flow stimulus, indicating that overall orientation behavior within groups was not consistent for the duration of flow presentation (Fig. 3b-c, Supplementary Table 3). Comparisons among groups within the initial 10s portion of flow showed a significant difference in the distribution of mean body angles between control and $CuSO_4$ fish, and between control and neomycin fish (Fig. 3b, Supplementary Table 3). There was also an interaction between treatment and stimulus where the distribution of mean body angle in $CuSO_4$-ablated fish during the initial stimulus bin was different than that of neomycin fish during the final sequence (Supplementary Table S3), suggesting that these lesion methods differentially impacted the rheotaxis behavior of fish.

Lateral Line-Ablated Fish Performed Rheotaxis for Shorter Durations but Travelled Longer Distances

Although intact lateral line was not required to perform rheotaxis, lesioned fish behaved differently than non-lesioned fish in flow stimulus, indicating that lack of input from neuromast hair cells affected swimming behavior. To quantify differences in rheotaxis behavior, we accounted for the random effects of individual variation then compared the mean duration and mean number of rheotaxis events, total distance travelled, and latency between flow presentation and behavior onset among groups. We standardized the data by comparing events of rheotaxis to events when fish were randomly oriented at 0° ± 45° under no flow and hereafter refer to both conditions as “events”.

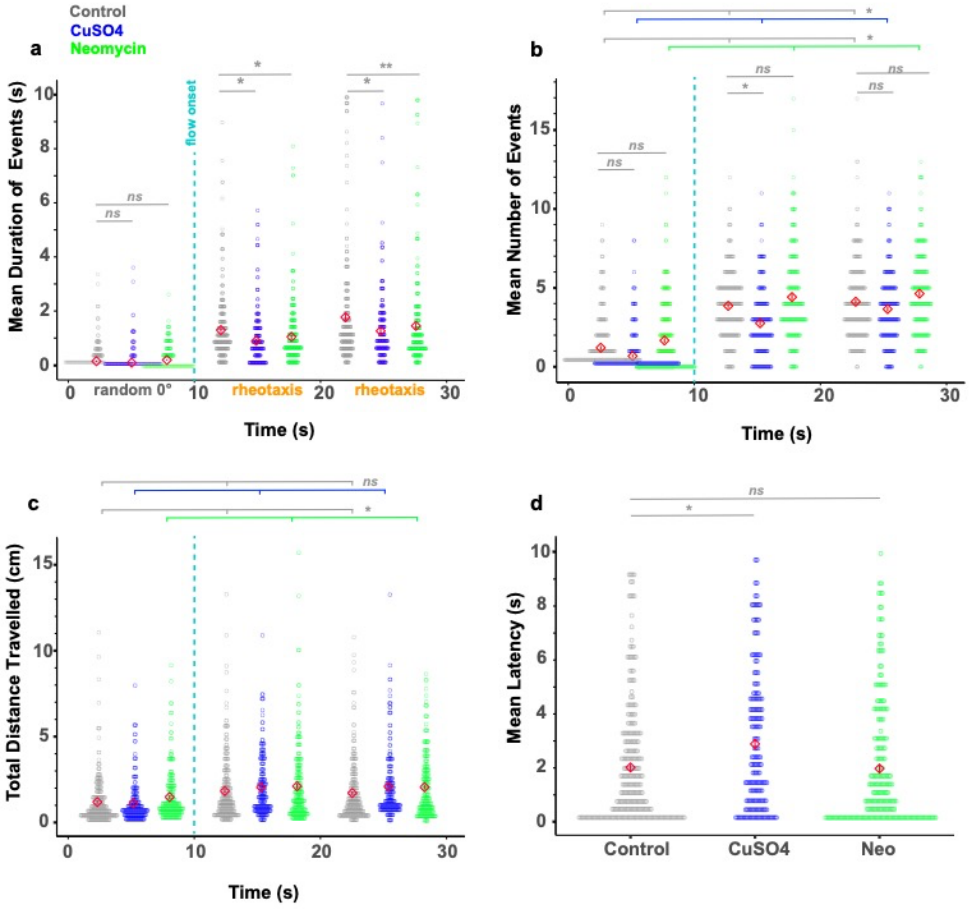

Figure 4. Lateral line ablated fish performed rheotaxis for shorter mean durations yet travelled greater total distances compared to controls. Red diamonds in each plot indicate the mean ± SE values. a) Lateral line intact (gray = control, n=248) fish have a longer mean duration of rheotaxis events during flow stimulus than lesioned fish (blue = $CuSO_4$, n = 204; green = neomycin, n = 222; 18 experimental sessions). b) The mean number of 0° orientation and rheotaxis events was greatest for neomycin fish and the least for $CuSO_4$ fish under no flow and flow conditions, respectively. c) Under no flow, neomycin fish traveled a greater total distance than control and $CuSO_4$ fish; but under flow, neomycin and $CuSO_4$ fish traveled a greater total distance than control fish. d) Compared to control and neomycin fish, $CuSO_4$ fish had the longest mean latency to the onset of the first rheotaxis event after flow stimulus presentation. Lines indicate statistical comparisons between control and treatment groups (see Supplementary Tables 4-7). The effects of treatment are indicated by long color-coded bars with branches, whereas interactions are indicated with short bars. There was a significant effect of stimulus in a-c (not shown for clarity). Significance values: * = 0.05, ** = 0.01

Without flow, the mean duration of random orientation events did not differ among treatment groups (Fig. 4a, Supplementary Table 4). With flow, the mean duration of rheotaxis events increased for each group, and was greatest in the controls, less in neomycin-, and least in $CuSO_4$-treated fish (Fig. 4a, Supplementary Table 4). An interaction between stimulus and

177 treatment was seen during the initial 10s of flow only in the $CuSO_4$ treatment cohort, but during
178 the final 10s the differences among all treatments became significant (Supplementary Table 4).
179 Mean number of events had a significant effect of stimulus and an effect of treatment where the
180 number of events was greatest in neomycin-treated, less in controls, and least in $CuSO_4$-treated
181 under no flow and flow conditions (Fig. 4b, Supplementary Table 5). The total distance travelled
182 during events was influenced by presence of flow stimulus and type of lesion, where neomycin-
183 treated fish travelled further than control and $CuSO_4$-treated fish in the presence or absence of
184 flow conditions (Fig. 4c, Supplementary Table 6). $CuSO_4$-lesioned fish also demonstrated a
185 greater delay in initiating rheotaxis compared to control and neomycin fish (Fig. 4d,
186 Supplementary Table S7). Altogether, our data show that an intact lateral line allowed fish to
187 sustain rheotaxis into oncoming flow for longer durations yet travel shorter distances,
188 suggesting that toxins reduce zebrafish economy of motion against flow stimulus. These results
189 support the idea that the lateral line allows epibenthic fish to hold their station with respect to the
190 substrate ([2], [33])

191 Interestingly, $CuSO_4$ and neomycin affected swimming behavior against flow stimulus in
192 different ways. $CuSO_4$ exposure decreased activity, as evidenced by fewer rheotaxis events
193 with greater latency between flow and behavior initiation. This contrasts with the neomycin-
194 exposed fish, that exhibited frequent bursts of rheotaxis, and longer distances travelled. We
195 propose that the distinct effects of $CuSO_4$ and neomycin treatments on the spatiotemporal
196 nature of rheotaxis may be due, in part, to their different mechanisms of neuromast ablation.
197 Hair cells were completely ablated and supporting cells and afferent neurons damaged at the
198 dosage used for $CuSO_4$ ([17]), but on occasion a few hair cells remained in neomycin-treated fish
199 (Supplementary Fig. 1). If residual hair cells retained some functionality in the neomycin group
200 despite severe morphological damage, then it is possible that their sensitivity might have been
201 amplified through efferent modulation ([34]) or previously silent hair cells were recruited to
202 compensate for reduced sensory input ([35]). In addition, while zebrafish larvae have been shown

to be relatively resistant to the concentration and exposure time of $CuSO_4$ used ([36]), subtle differences in behavior may also be a consequence of nonspecific neural toxicity.

Overall Spatial Use of the Arena During Rheotaxis Differs Among Treatments

During flow, we observed that lateral line-lesioned fish were often pushed against the back of the testing arena, whereas intact fish were often swimming at the front of the arena near the flow source. To quantify this observation, the density of fish throughout the duration of the experiment was plotted in one- and two-dimensional (1D, 2D) space and then compared among treatments.

Along the X-axis, the spatial use was similar among treatment groups and flow conditions (Fig. 5a). All groups preferred the sides over the middle of the arena. Without flow, fish that were placed into the arena remained close to the walls as they explored the boundaries. With flow, preference for the sides became more pronounced due to gradients in the laminar flow field where the highest velocities occurred at the surface and left side and the lowest velocities at the bottom and right side (Supplementary Fig. 2). These boundary layers provided a refuge (e.g. [37]) for intact and lesioned fish alike to reduce their energetic costs ([38]).

By contrast, the spatial use of fish along the Y-axis differed significantly among treatment groups and became more prominent during flow conditions (Fig. 5b). Under flow, the control group predominantly used the front region (Fig. 5b), demonstrating that an intact lateral line allowed these fish to maintain their position at the front of the arena where the flow was strongest. Conversely, the predominant location of toxin-treated groups was shifted toward the back region, suggesting an impaired ability to station hold and increased reliance on tactile cues provided by contact with the rear grate. $CuSO_4$-lesioned fish exhibited a greater shift towards the back of the arena than neomycin-lesioned fish (Fig. 5b), but both groups demonstrated this abnormal distribution along the Y-axis compared to control fish.

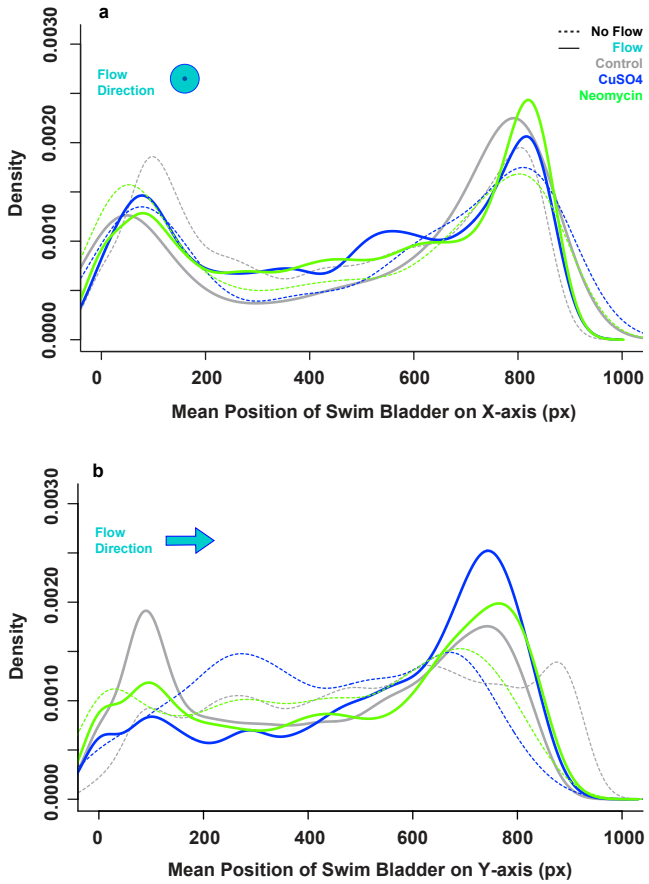

Figure 5. Intact lateral line allowed fish to hold their position near the source of the flow. a) The total spatial use of the arena in the X- dimension (left to right) does not differ among treatments (gray = control, blue = $CuSO_4$, green = neomycin) or flow conditions (none = dotted lines, flow = solid lines). All fish preferred to occupy the right versus the left side of the arena. b) in the Y- dimension (front to back) under no flow conditions, the $CuSO_4$ treated fish occupied the center of the arena more than the control or neomycin treated fish. However, under flow conditions, the lateral line intact (control; gray solid line) fish occupied the front of the arena, whereas lesioned fish (blue and green solids lines) predominantly occupied the back of the arena.

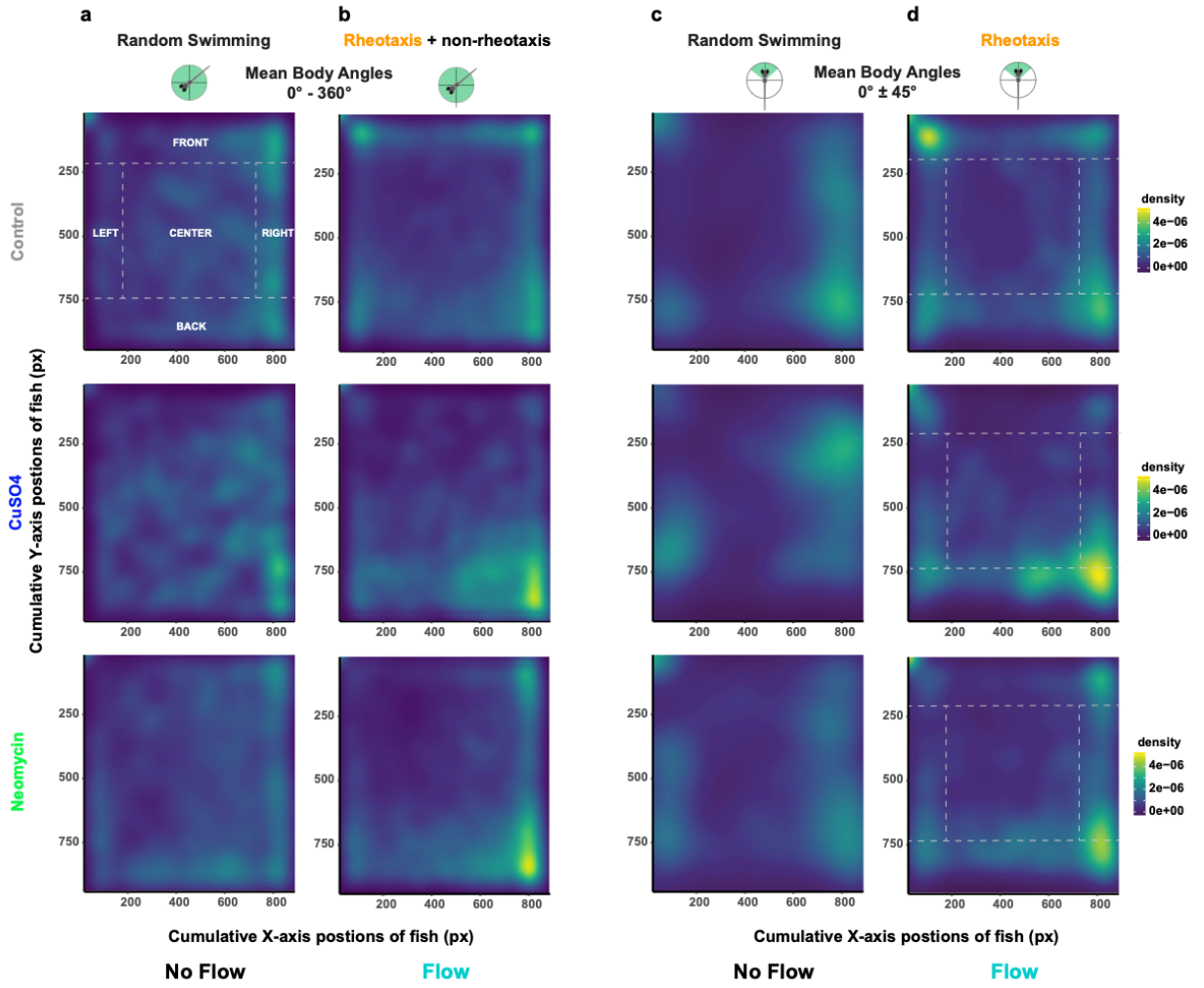

Figure 6. Under flow, lateral line intact (control) fish used the front part of the arena near the source of the flow, whereas lesioned (CuSO4, neomycin) fish use the back portion of the arena. a-b) For all possible mean body angles (0°- 360°): a) all treatment groups of fish show similar density, or total spatial use, of the arena under no flow conditions; b) however, the controls used the front of the arena and the lesioned fish used the back of the arena under flow. c-d) Filtering the data for mean body angles required for rheotaxis (0° ± 45°): c) all groups clustered along the left and right sides of the arena under no flow; d) but under flow, the controls used the front-left and the lesioned use the back-right portions of the arena. Dotted lines and labels in capital letters indicate spatial regions of interest (ROI). For clarity, statistical comparisons among treatment and ROIs were not included in the figure; however, there were significant fixed effects for CuSO4 and neomycin treatments, the back ROI, and interactions between treatment and ROI (Supplementary Table 8).

The spatial use of the arena in 2D further illustrates differences among treatment groups under flow. During rheotaxis, the total density of fish in 2D space was parsed out over five regions of interest (ROI, Fig. 6a) set according to size of fish, their orientation during rheotaxis, and the dimensions of the flow field. Generalized linear models (Supplementary Table 8)

indicate that the spatial use of fish during rheotaxis differed among all three treatment groups. (Fig. 6d). During flow, control fish frequently maintained position in the upper-left corner of the arena whereas lesioned fish primarily occupied the back-right corner (Fig. 6d), suggesting that a functional lateral line enables fish to occupy the areas of strongest flow. The propensity of lesioned fish to be swept backwards yet still perform rheotaxis behavior without visual cues likely demonstrates that they relied on tactile cues to provide the external frame of reference necessary to orient and swim against flow ([2], [8], [10]). Cumulatively, these observations support that the sensory information provided by lateral line organs, in conjunction with the tactile system, allowed intact fish to actively maintain their position within a non-uniform laminar flow field where the velocity of water is greatest ([2]).

Lateral Line Ablation Reduces the Proportion of Individual Fish that Perform Rheotaxis

During flow presentation, the control group had the greatest proportion of individual fish that performed rheotaxis during the experiment (as defined in Fig. 2) followed by neomycin-treated then $CuSO_4$-treated groups (Fig. 7). Intact fish plateaued relatively quickly compared to lesioned fish, but the values for all three groups converged during the final few seconds of flow presentation.

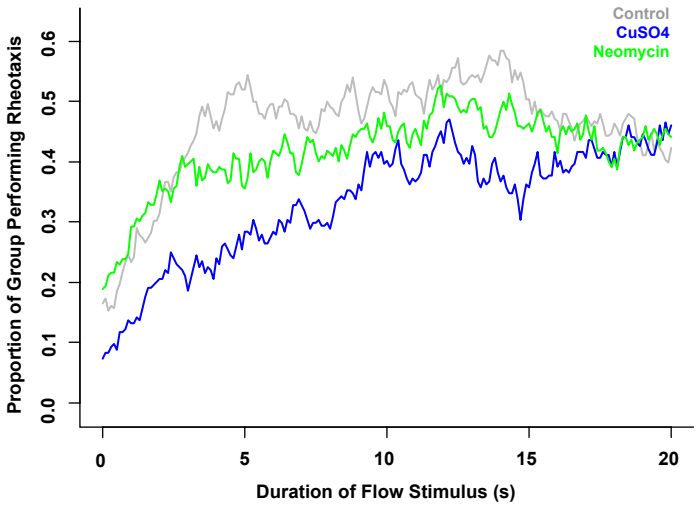

Figure 7. Intact lateral line enabled a greater proportion of fish to perform rheotaxis within the first 15 seconds of stimulus onset. Time series of the proportion of individual fish within each group that performed rheotaxis during flow presentation. A greater proportion of lateral line intact (gray = control) fish performed rheotaxis than lesioned (blue = $CuSO_4$, green = neomycin) fish. The data for all treatments converges after 17 s of flow presentation.

Spectral Decomposition Shows that Lateral Line Ablation Impacts the Trend and Degree of Periodic Fluctuation in Linear and Angular Movement

To uncover the impact that lateral line ablation had on the swimming kinematics of fish, we analyzed how the magnitude of the linear (relative distanced moved, relative velocity, relative acceleration) and angular movements (mean body angle, mean length of the resultant vector) changed over time. We observed that all treatment groups swam in the burst-and-glide style that is characteristic of larval zebrafish with intact lateral lines, but with noticeable differences in the quality of their movement. Because the lateral line is thought to mediate station holding behavior ([2], [33], [38]), we postulated that, under flow, the magnitude of the oscillations in relative linear and angular movements of lateral line-intact fish would be smaller than those of lesioned fish. The observed time series data (Fig. 8a, d, g; Supplementary Fig. 3 a, d) had a “seismic” appearance where noise masked the underlying signal. Therefore, we removed the random noise (Supplementary Fig. 3g-k) and decomposed the observed datasets into their fundamental components: the large scale trends in the magnitude of movements during the entire experiment (Fig. 8b, e, h; Supplementary Fig. 3 b, e) and the small scale periodicity, which indicates the recurring fluctuations in movement magnitude that occurred during any given second of the experiment (Fig. 8c, f, i). Only relative movement data are shown in Fig. 8 to provide visual clarity because the relative velocity and acceleration periodicity data showed similar fluctuations (Supplementary Fig. 3 c, f).

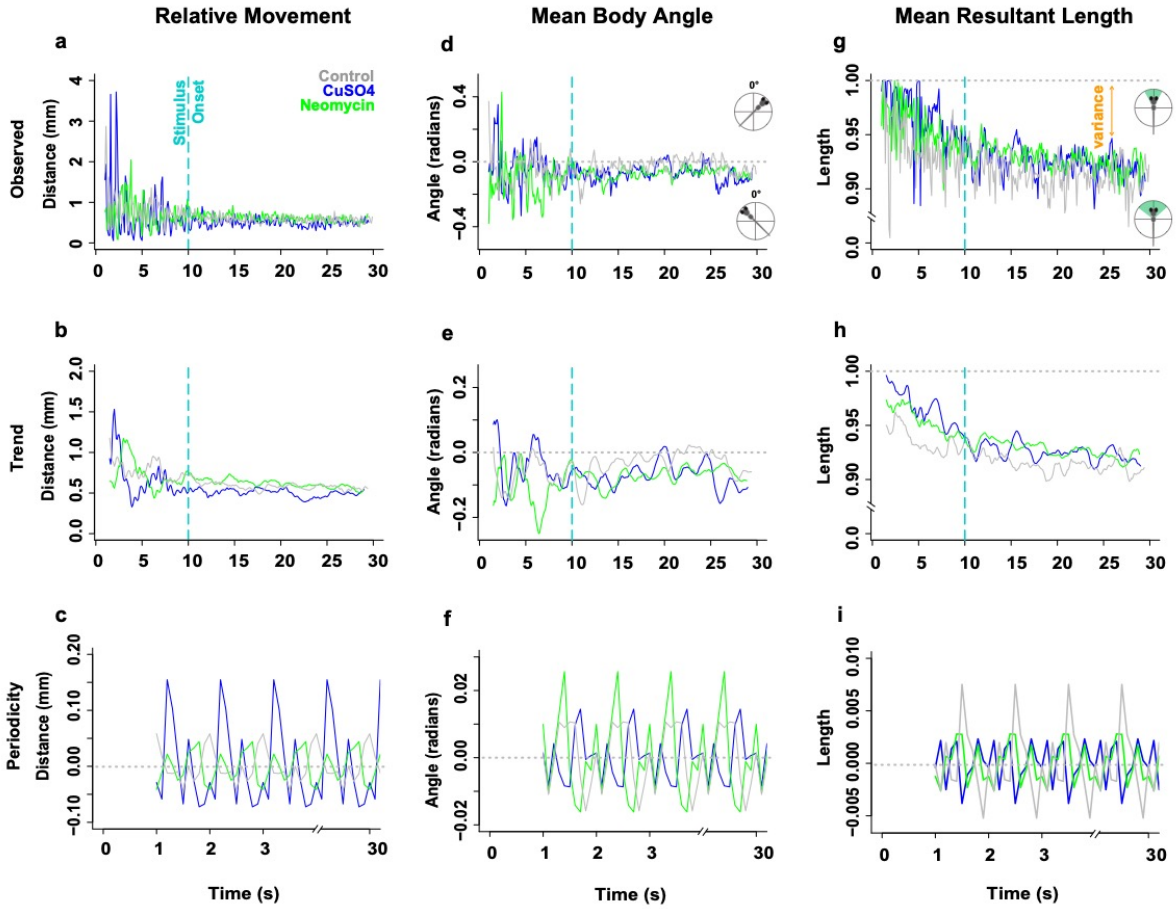

Figure 8. The overall trends and periodic fluctuations in the linear (relative distance moved) and angular (mean body angle, mean length of the resultant vector) motion parameters of rheotaxis behavior differ among treatment groups. (Note: the relative velocity and acceleration periodicity data mimicked the patterns observed in relative movement; see Supplementary Fig. 3). Gray = control, blue = $CuSO_4$, green = neomycin. Spectral decomposition of the observed data (a, d, g) removed the noise (Supplementary Fig. 3g, h, i) to reveal the overall underlying trends (b, e, h) and the periodicity, or recurring fluctuations (c, f, i) that occurred during any given 1 s of the experiment. The periodicity waveform peaks (c, f, i) indicate the average amount (amplitude), number, direction (positive = increasing; negative = decreasing), and order of occurrence for these cyclic fluctuations as a function of unit time (1 s). The overall trends were that $CuSO_4$ treated fish had the least relative movement (b), while the control fish more rapidly oriented to 0° (e) and swam with more angular variance (h; 1 – mean length of the resultant vector) compared to lesioned fish. The periodic fluctuation in relative distance moved (c) was greatest in $CuSO_4$ treated fish compared to control or neomycin treated fish. However, the fluctuation in mean body angle (f) was greatest in neomycin treated fish compared to control and $CuSO_4$ fish, while the fluctuation in mean length of the resultant vector (i.e the angular variance; i) was greatest in control fish compared to lesioned fish.

During rheotaxis, the trend among groups was that $CuSO_4$ ablation reduced the magnitude of relative movement (Fig. 8b) but not the relative velocity or acceleration of fish (Supplementary Fig. 3 c, f) compared to control and neomycin groups. For the trends in angular

311 movements, $CuSO_4$- and neomycin-treated fish showed a reduced ability to achieve and
312 maintain orientation with flow compared to controls (Fig. 8e). Lesioned fish had longer mean
313 resultant vector lengths and greater fidelity to a mean body angle compared to controls (Fig. 8h)
314 which swam with more angular variance (1- *rho*) than lesioned fish. Consequently, an intact
315 lateral line allowed control fish to detect minute changes in water flow and make regular course
316 corrections of small magnitude, thereby increasing their angular variance (Fig. 8h) and enabling
317 them to rapidly orient into flow with greater accuracy (Fig. 8e) and led to a greater proportion of
318 non-lesioned fish performing rheotaxis compared to lesioned fish (Fig. 7).
319 Among treatment groups, there were clear differences in the periodicity of the changes
320 in the magnitude of linear (Fig. 8c; Supplementary Fig. 3 c, f) and angular (Fig. 8f, i)
321 movements. The linear periodicity data showed that $CuSO_4$-treated fish had the greatest
322 fluctuation in the magnitude of their relative distance moved, velocity, and acceleration
323 compared to the control and neomycin-treated fish (Fig. 8c; Supplementary Fig. 3 c, f;
324 Supplementary Table 9). Conversely, the neomycin-treated fish had the lowest fluctuations in
325 the magnitude of their linear movements. The large magnitude of the periodic oscillations in
326 $CuSO_4$-treated fish could compensate for their delayed response to flow (Fig. 4d), reduced trend
327 in relative movement (Fig. 8b), and explain the relative increase observed in total distance
328 traveled during flow (Fig. 4c). Furthermore, $CuSO_4$-treated fish had large amplitude peaks that
329 occurred early during the random sampling periods, whereas neomycin-treated and control fish
330 had smaller peaks that increased gradually (Fig. 8c; Supplementary Fig. 3 c, f). These empirical
331 data support the qualitative observations that $CuSO_4$ ablation resulted in fish that performed
332 rheotaxis with delayed responses and erratic movements. Additionally, the maxima in control
333 fish occurred at the end of the sampling period (Fig. 8c), indicating an intact lateral line allowed
334 fish to exhibit a graded and more controlled response to flow compared to lesioned fish.
335 The range in amplitude of the angular periodicity data showed a different pattern where
336 neomycin-treated fish had the greatest fluctuation in mean body angle, followed by the controls,

and then the $CuSO_4$-treated fish (Fig. 8f; Supplementary Table 9). Notably, all three treatment groups had a small dip and correction during the initial portion of the sampling period (Fig. 8f), which indicates that all fish had the same initial small change in mean body angle to the left of the flow. Control and $CuSO_4$-treated fish had a subsequent series of minor heading changes to the right (positive values) and left (negative values) of the flow, whereas the neomycin-treated fish regularly overshot their initial and secondary responses before recovering. These large oscillations might explain why neomycin fish had difficulty locking onto the source of the water flow (Fig. 8e). However, the smaller fluctuations in mean body angle observed in control and $CuSO_4$-treated fish (Fig. 8f) is not sufficient to explain why control fish could rapidly and consistently orient toward the flow better than $CuSO_4$-treated fish (Fig. 8e). Perhaps the greater variety of temporal fluctuation combined with the small amplitude fluctuations allowed intact fish to more rapidly attune their mean body angle to the flow compared to $CuSO_4$ fish (Fig. 9d; see *Spectral Analysis*). In both neomycin- and $CuSO_4$- lesioned fish, the waveform structure for the mean resultant length per second shows a rapid succession of several small peaks, but that of control fish has two small peaks followed by two large peaks (Fig. 8i). These small initial changes in angular variance of intact fish might reflect greater capacity to sample flow stimuli from a variety of small angles to produce large correctional changes in angular variance (Fig. 8i) with better efficacy (Fig. 8e).

Spectral Analysis Reveals that Lateral Line Ablation Impacts the Temporal Fluctuation of Linear and Angular Movement

The fluctuations in periodicity data have a predictable and repeatable temporal structure that can be described by a series of fundamental sine and cosine functions that oscillate at different frequencies (Hz; cycles s^{-1}) and periods (s $cycle^{-1}$). Therefore, we performed a spectral analysis to decompose the periodicity data (Fig. 8c, f, i; Supplementary Fig. 3 c, f) and determine the fundamental frequencies at which the fluctuations in linear and angular

363 movement occurred (Fig. 9a-e). For the power spectra of each parameter, the frequency and
364 amplitude of three most dominant peaks were summed to calculate the net shifts in frequency
365 and power among treatment groups (Supplementary Table 10).

366 Relative to controls, the overall trend in lesioned fish was a net downshift in the
367 dominant frequencies of relative movement, velocity, and acceleration, a net upshift in the mean
368 body angle, and a net increase in amplitude across these four parameters (Fig. 9a-d,
369 Supplementary Table 10). This indicates that lateral line-ablated fish swam with less frequent
370 changes in their linear movements, more frequent changes in their mean body angle, and
371 greater numbers of movements at these frequencies relative to controls. The curves for mean
372 resultant vector length showed a notable difference between the two ablation treatments where
373 $CuSO_4$-treated fish had a net frequency downshift and a net amplitude increase relative to
374 controls (Fig. 9e, Supplementary Table 10), and vice versa for neomycin-treated fish (Fig. 9e,
375 Supplementary Table 10). Therefore, $CuSO_4$-lesioned fish swam with more low frequency
376 changes in angular variance, while neomycin-lesioned fish swam with fewer high frequency
377 changes in angular variance.
378

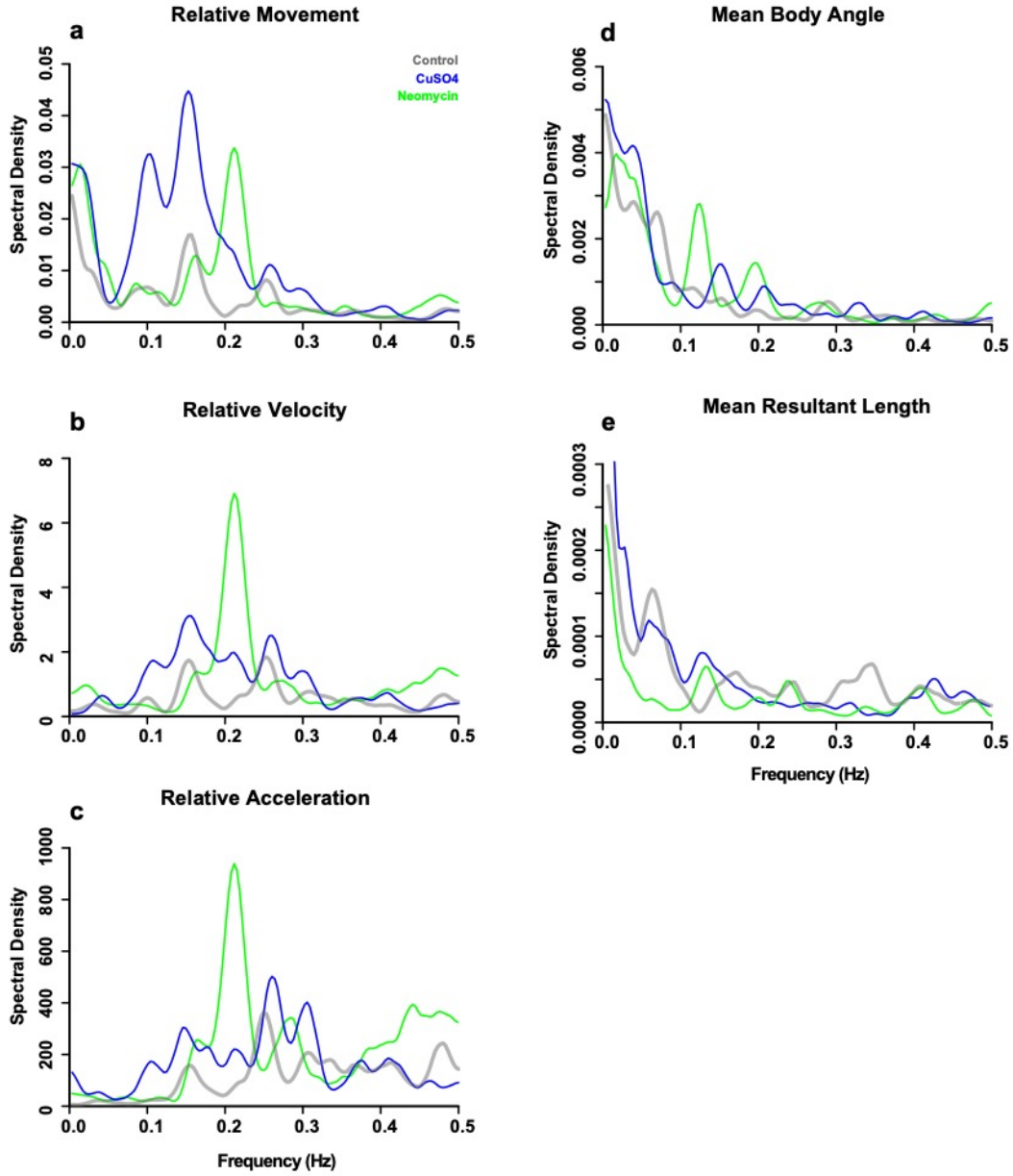

Figure 9. Power spectra density curves show that an intact lateral line allowed fish to make fewer yet more temporally variable changes in relative linear and angular movement. Because frequency and period are inversely related, the low frequency peaks to left of the periodograms indicate cycles with longer periods, and vice versa The amplitude of the peaks indicates the spectral density, or the number of movement events at a given frequency that occurred during the experiment. The peaks with the greatest amplitude indicate the fundamental or dominant frequencies of fluctuation in the periodicity data. The frequency and amplitude of three most dominant peaks were summed to calculate the net shifts in frequency and power. Relative to controls (gray), lesioned (blue = $CuSO_4$, green = neomycin) fish had a net downshift in the three dominant frequencies of (a) relative movement, (b) velocity, and (c) acceleration and a net upshift in (d) mean body angle of larval zebrafish during rheotaxis. For the dominant frequencies of (e) mean resultant length, there was a net downshift and upshift for $CuSO_4$- and neomycin-treated fish, respectively. Furthermore, relative to lateral line intact fish, the peaks of lesioned fish are clustered into fewer peaks of greater

amplitude over a relatively narrow range, which indicates that lateral line ablation increased the number yet reduced the temporal variation of changes in movement.

Compared to neomycin-treated fish, the power spectra of the linear movements in control and $CuSO_4$-treated fish (Fig. 9a-c) show broad clusters of dominant peaks that gradually upshift with each subsequent time derivative. $CuSO_4$-treated fish swam with the greatest number of low-frequency fluctuations in relative movement, but the fluctuations in their velocity and acceleration had greater temporal variety and occurred with increasing frequency in a manner similar to those of control fish. Interestingly, the curves for linear movement in neomycin-treated fish are dominated by a single peak at the primary frequency of 0.21 Hz that remained constant with each time derivative (Fig. 9a-c). Therefore, neomycin ablation reduced the temporal variation of the cyclic fluctuations in relative movement, velocity, and acceleration of fish during rheotaxis. This clustering of rheotaxis behaviors into fewer peak responses with discrete timing, or temporal contraction, was further seen in the angular power spectra of lesioned fish. For example, the power spectrum of the mean body angle in control fish is relatively flat with small peaks, whereas those of ablated fish are focused into distinct dominant frequencies with larger amplitudes (Fig. 9d; also see Fig. 8f). Likewise, the spectrum of the mean resultant length in controls shows five broadly spaced peaks, but those of the lesioned fish are clustered into fewer peaks focused at the dominant frequencies (Fig. 9e). Therefore, intact fish swam with fewer overall changes to their mean body angle, but their angular variance had greater temporal variety (Fig. 9e) and magnitude (Fig. 8h, i) compared to lesioned fish.

We interpret the relatively flat and generally lower peaks observed in the power spectra of control fish (Fig. 9a-d) as indicating that sensory data from the lateral line allowed fish to make fewer changes in linear and angular movement over a broader range of frequencies, thus increasing the efficiency and efficacy of their response to flow. Conversely, fewer peaks of greater amplitude observed in lesioned fish indicate that loss of mechanosensory input from the

lateral line resulted in greater numbers of swimming adjustments that were temporally restricted, reducing their economy of movement within flow.

Cross Correlation Between Linear and Angular Movements Shows Distinct Rheotaxis Profiles Among Groups

Changes in linear movement may be temporally cross-correlated with changes in angular movement, depicting rapid turns in response to flow. As these movements receive input from the lateral line, we investigated the effect of toxins on cross correlation between linear and angular movements. The correlograms depict how an above average increase in relative movement (Fig. 10a-b), velocity (Fig. 10c-d), or acceleration (Fig. 10e-f) cross-correlates with above average changes in the mean body angle (Fig. 10a, c, e) or mean resultant length (Fig. 10b, d, f).

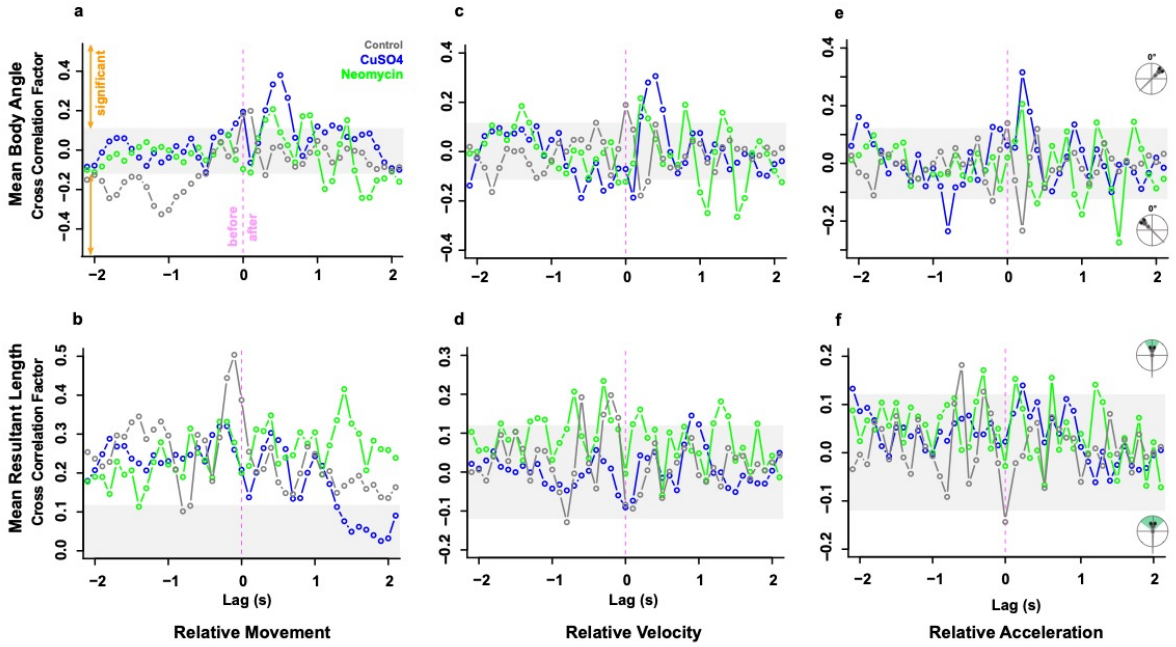

Figure 10. Cross correlations between linear and angular movement data indicate toxin-specific changes to the rheotaxis behavioral profile of fish. The correlograms depict how an above average increase in relative movement (a, b), relative velocity (c, d), or relative acceleration (e, f) were significantly cross-correlated with above average increases or decreases in the mean body angle (a, c, e) or mean resultant length (b, d, f). In the figures for mean body angle (a,c,e), the positive and negative peaks indicate that fish were oriented to the right or left of the oncoming flow vector, respectively. In the figures for mean resultant length (b, d, f),

the positive and negative peaks indicate fish that had a lesser or greater variance of the mean body angle, respectively. The X-axis indicates the relative timing, or lag, of the cross correlation between the angular parameter with respect to an above average increase in the linear parameter (zero = simultaneous occurrence; negative = angular change occurs *before* linear change; and positive = angular change occurs *after* linear change). *For example, interpret panel 10a as:* In control (gray) fish, above average increases in relative movement are significantly correlated with changes in mean body angle to the left of the flow vector that previously occurred. In $CuSO_4$-treated (blue) fish, above average increases in relative movement are significantly correlated with above average changes in mean body angle that subsequently occurred. In neomycin-treated (green) fish, above average increases in relative movement are significantly correlated with below average changes in mean body angle that subsequently occurred.

Focusing on the strongest cross-correlations (Fig. 10; Supplementary Table 11) shows three distinct patterns in the direction and relative timing of changes between mean body angle and linear movements (Fig. 10a, c, e) and between temporal changes in angular variance and linear movements (Fig. 10b, d, f). In controls, the changes in body angle direction and the timing between angular and linear movements were temporally cross correlated, producing smooth re-orienting movements characteristic of effective station holding during rheotaxis (Fig. 10a, c, e). In addition, control fish tended to *reduce* their angular variance *prior* to a large change in movement (Fig. 10b), velocity (Fig. 10d), or acceleration (Fig. 10f). Therefore, the relative timing and direction of changes in mean body angle in lateral line-intact fish depended upon the time derivative of the linear movement, but the relative timing between reduced angular variance was consistent across changes in all linear movements.

In lesioned fish, the timing and direction of the strongest cross-correlations shifted the rheotaxis profile of these fish in a predictable, consistent, and treatment-specific manner. $CuSO_4$ fish tended to change their mean body angle to the *right* of the oncoming flow vector *after* large changes in movement (Fig. 10a), velocity (Fig. 10c), and acceleration (Fig. 10e). However, neomycin fish tended to change their body angle to the *left* of the flow *after* changes in movement (Fig. 10a), velocity (Fig. 10c), and acceleration (Fig. 10e). As in controls, lesioned fish always *reduced* their angular variance when changing their linear movements, but the relative timing of the cross-correlation shifted according to the toxin used and the time derivative of the linear movement. In $CuSO_4$-treated fish, the strongest correlation between a *reduction* in

463 angular variance tended to occur *prior* to changes in movement (Fig. 10b), *after* changes in
464 velocity (Fig. 10d), and *after* changes in acceleration (Fig. 10f). Conversely, in neomycin-treated
465 fish, *reductions* in angular variance occurred *after* changes in movement (Fig. 10b), *before*
466 changes in velocity (Fig. 10d), and *before* changes in acceleration (Fig. 10f).
467 These data revealed that control fish with intact lateral line detected oncoming flow and
468 adjusted their mean body angle *prior* to making a change in their relative movement, while
469 lateral-line lesioned fish changed their mean body angle *after* a change in their relative
470 movement. We posit that an intact lateral line allowed fish to rapidly detect flow and adjust their
471 heading prior to swimming into the flow while, in the absence of visual and lateral line cues,
472 lesioned fish had to rely on tactile cues, such as physical displacement along the substrate, to
473 gain an external frame of reference necessary to orient and swim into flow. Intact fish also
474 tended to change their body angle to the left of the flow vector, which might reflect lateral line
475 handedness where larval zebrafish prefer to use the right side of their lateral line to detect flow
476 stimuli in a manner similar to that of blind cavefish ([39]). This undoubtedly shifted the relative
477 timing of the cross-correlations between angular and linear movement, perhaps impaired any
478 potential lateral line handedness, and further contributed to the erratic rheotaxis behavior
479 observed in these fish.
480 In summary, lateral line ablation of larval zebrafish resulted in distinct, treatment-specific
481 rheotaxis profiles that differed from that of intact fish in the following ways: 1) delayed relative
482 timing between changes in mean body angle and all linear movements, 2) changed mean body
483 angle in response to flow, and 3) shifted timing between reductions in angular variance and
484 changes in linear movement.
485
486 **CONCLUSIONS**
487 In this study, ablating the lateral line of larval zebrafish with two commonly used toxins
488 impacted their ability to produce the fine adjustments required to station hold in response to

water flow. Lateral line ablation inhibited the ability of fish to discriminate subtle distinctions in flow, resulting in more intense overcorrections and decreased economy of motion. Our data support the hypotheses that the lateral line mediates station holding behavior ([2], [33], [38]), but is not required for rheotaxis behavior ([2], [11], [12], [29], [30]) in larval zebrafish in non-uniform laminar flow. We posit that the physical displacement of lesioned fish along the substrate provided sufficient tactile cues ([8], [10]) necessary for lateral line ablated fish to perform rheotaxis.

We propose that the greater angular variance observed in intact fish might indicate that these fish were regularly sampling the velocity gradients of the flow stimuli ([22]) from a variety of body angles so that they could reduce their response latency, quickly orient with respect to fluctuating flow stimuli, and maintain their overall mean body angle with greater fidelity to the flow vector than lesioned fish. During flow, intact fish had recurring fluctuations in relative movement, velocity, and mean body of lower magnitude, and fluctuations in relative movement, velocity, acceleration, and mean body angle of controls that were fewer in number yet occurred over a wider range of temporal frequencies compared to lesioned fish. Thus, the sensory cues detected by the lateral line allowed control fish to respond to water flow with less intensity and greater temporal variation in their movements, resulting in greater economy of movement.

This is the first study to demonstrate that two toxins commonly used to ablate the lateral line impacts the behavioral profiles and mechanism of rheotaxis in zebrafish. We propose a novel functional assay for hair cell ototoxicity, which may be used to supplement future studies exploring lateral line injury, protection, and recovery. Furthermore, the simplicity of the equipment and precision of the machine learning analyses used in this assay make it amenable to adaptation for detecting subtle behavioral changes in a wide variety of animal models.

METHODS

Ethics Statement

514 This study was performed with the approval of the Institutional Animal Care and Use
515 Committee of Washington University School of Medicine in St. Louis and in accordance with
516 NIH guidelines for use of zebrafish.

517

518 *Zebrafish*

519 Adult zebrafish were raised under standard conditions at 27-29°C in the Washington
520 University Zebrafish Facility. The wild type line AB* was used for all experiments unless
521 otherwise stated. Embryos were raised in incubators at 28°C in E3 media (5 mM NaCl, 0.17 mM
522 KCl, 0.33 mM $CaCl_2$, 0.33 mM $MgCl_{2;}$ ([40])) with a 14:10 hr light:dark cycle. After 4 days post
523 fertilization (dpf), larvae were raised in 100-200 mL E3 media in 250-mL plastic beakers and fed
524 rotifers daily. Sex of the animal was not considered in our study because it cannot be
525 determined in larval zebrafish.

526

527 *Lateral Line Ablation*

528 At 6 or 7dpf, ~15 larval zebrafish were placed into each well of a flat bottom 6-well
529 polystyrene plate (#351146, Falcon) in 8 mL of E3 media. Treatment animals were placed into
530 50 µM neomycin trisulfate salt hydrate (N1876-25G, Sigma Aldrich) or 10 µM $CuSO_4$ (451657-
531 10G, Sigma Aldrich) solutions made in 8 mL of E3 media. The plate was placed into an
532 incubator at 29°C and exposed to the treatment for 30 min (neomycin) or 60 min ($CuSO_4$). After
533 exposure, the fish were removed from treatment, rinsed 3X in media, then placed into 8 mL of
534 clean media and allowed to recover for 120 min ($CuSO_4$) or 150 min (neomycin) in the
535 incubator. Recovery times for $CuSO_4$ and neomycin were chosen to standardize the total time of
536 treatment and recovery to 180 min. Control fish (n = 248) received no chemical treatments yet
537 underwent the same procedures as the $CuSO_4$ (n = 204) and neomycin (n = 222) fish. At the

538 end of treatment, the larvae were removed from the incubator and immediately began rheotaxis
539 behavior trials.

540

541 *Immunohistochemistry*

542 Lateral line ablation was confirmed via immunohistochemistry on a subset of control and
543 lesioned fish. Larvae were sedated on ice (5 min, 0°C) then fixed overnight at 4°C in PO_4 buffer
544 with 4% paraformaldehyde, 4% sucrose, and 0.2 mM $CaCl_2$. Larvae were rinsed 3X with PBS
545 and blocked for 2 hr at room temperature in PBS buffer with 5% horse serum, 1% Triton-X, and
546 1% DMSO. Primary antibodies for Otoferlin (HCS-1, Developmental Studies Hybridoma Bank,
547 mouse IgG2a, 1:500) were diluted in 1x PBS buffer with 2% horse serum and 0.1% Triton-X,
548 then incubated with the larvae overnight at 4°C with rotation. Larvae were rinsed 5X with PBS
549 solution, then placed in secondary antibody (ThermoFisher, goat anti-mouse IgG2a, Alexa 488,
550 1:1000) diluted in PBS with 2% horse serum and incubated for 2 hr at 22°C with rotation. Fish
551 were rinsed 3X with PBS then incubated with DAPI (Invitrogen, 1:2000) in PBS for 20 min at
552 22°C to label cell nuclei. Larvae were rinsed 2X with PBS then mounted onto glass slides with
553 elvanol (13% w/v polyvinyl alcohol, 33% w/v glycerol, 1% w/v DABCO (1,4 diazobicylo[2,2,2]
554 octane) in 0.2 M Tris, pH 8.5) and #1.5 cover slips.

555

556 *Confocal Imaging and Processing*

557 Immunolabeled z-stack images were acquired via an ORCA-Flash 4.0 V3 camera
558 (Hamamatsu) using a Leica DM6 Fixed Stage microscope with an X-Light V2TP spinning disc
559 confocal (60 µm pinholes) controlled by Metamorph software. The region of interest tool in
560 Metamorph was used to select specific neuromasts (~700 x 700 px) from the surrounding area.
561 Z-stack images of 100 ms exposure were acquired through with a 10X/0.3 N.A. dry lens in 2 µm
562 slices or through a 63X/1.4 N.A. oil immersion lens 0.5 µm slices. Excitation for DAPI (405 nm)

and Alexa 488 GFP was provided by 89 North LDI-7 Laser Diode Illuminator on the lowest power setting (20%) that could acquire images and minimize photobleaching. Confocal images were processed in FIJI (ImageJ, NIH) software to create maximal z-stack maximal projection composite images with minor exposure and contrast adjustments. Composite images were stitched together in Adobe Photoshop CC.

Experimental Apparatus for Rheotaxis Behavior

A microflume (220 x 100 x 40 mm; Fig. 1a) was constructed in two pieces from clear resin (RS-F2-GPCL-04, Formlabs) using a high-resolution 3D printer (Form 2, Formlabs) and joined with two-stage epoxy. A 1 mm-thick top layer of plastic was cemented with silicone sealant downstream of the flume pump (Fig. 1a) to prevent water spillage out of the apparatus. The low-pressure portion of the flume away from the flume pump remained open at the top to facilitate the addition and removal of water and fish when necessary. A square (30 x 30 x 10 mm) arena was 3D printed from clear resin and 25 µm mesh was cemented with epoxy on to the open upstream and downstream sides, allowing water to flow through the working section. The arena served to isolate larval fish at a specific location within the flume, enabling reliable video recording. A 6V bow thruster motor (108-01, Raboesch) was inserted into the flume (Fig. 1b) and used to pump water through the flume at a constant velocity. The water pump was connected to a 7.2 V power supply and the flow rate was modulated by an inline rheostat. An Arduino (UNO R3, Osepp) with a digital display using custom scripts was used to control and monitor the onset and duration of water flow in a consistent manner.

Rheotaxis is a multimodal behavior that is mediated by the visual, vestibular, mechanotactile, and lateral line systems. It was not possible to selectively block the detection of tactile cues in a non-invasive manner. However, evidence suggests that the angular motion in the horizontal plane (i.e. yaw) is not detectible in larval zebrafish at 6-7dpf ([31], [32]), and we

588 reduced linear acceleration cues to the vestibular system by using a flow stimulus of that rapidly
589 accelerated (< 250 ms) to a constant maximum velocity (V = 9.74 mm s-1). We further isolated
590 the contribution of the lateral line to rheotaxis by performing the rheotaxis assay under infrared
591 light to eliminate visual cues (Fig. 1a). The flume was placed onto a diffused lighting array of
592 196 LEDs that emitted infrared (IR) light at 850 nm upward through the translucent flume (Fig.
593 1b). A monochromatic high speed camera (SC1, Edgertronic.com) without an IR filter was
594 placed on a weighted tripod directly over the flume to record behavioral trials at the following
595 settings for optimal speed of data acquisition and machine learning analyses: either 200 or 60
596 frames s^{-1} (fps), ISO 20,000, and 1/1000 s shutter speed. The 60 mm Nikon macro lens was
597 manually set to an aperture of *f*16 to ensure adequate depth of field. The live video feed was
598 monitored on the PC and video recordings were remotely triggered by the Arduino. Videos of
599 each trial were recorded onto 64 GB SD cards for subsequent archiving in duplicate onto a 10
600 TB RAID array (Mercury Elite Pro Dock, OWC).

601

602 *Rheotaxis Behavior Pre-trial Preparation*

603 The camera was connected to the local area network (LAN) and initialized according to
604 the manufacturer procedure (http://wiki.edgertronic.com/index.php/Quick_start_guide). A layer
605 of light diffusing material (several Kimwipes© in a sealed plastic sheath) was placed on top of
606 the IR light array. The flume was placed on the diffusion material and filled with E3 media (28°C)
607 and the arena was then placed within the flume. The camera height over the flume was
608 determined by the maximum image size of the arena within the video frame that allowed a ~10-
609 20 pixel border for subsequent cropping during video pre-processing. Because IR light is a
610 significant source of heat, a thermometer was placed into the open portion of the flume and mini
611 frozen ice packs (2 x 2 cm; -20°C) were used to maintain a consistent temperature range of 27-
612 29°C.

Rheotaxis Trials

Under IR illumination, a single larval zebrafish was transferred by pipette from the 6-well plate to the arena in the flume. The swimming activity of the fish was monitored for ~10 s to ensure that it exhibited the burst-and-glide behavior indicative of normal larval zebrafish swimming ([41]). The Arduino was activated, and the trial began by recording 10 s of baseline swimming behavior on video. After 10 s had elapsed, the flume pump was automatically activated for 20 s and delivered a constant mean (± SD) water flow stimulus of 9.74 ± 1.43 mm s^{-1} (approximately 2 larval fish body lengths s^{-1}) while the camera continued to record swimming behavior. After a total of 30 s (no flow = 0-10 s; initial flow = 10-20 s; and final flow = 20-30 s) had elapsed, the pump turned off, the camera stopped recoding, the file was saved to the SD card, and the larvae was removed from the arena. Cohorts of five individual fish from each group (control, neomycin, or $CuSO_4$) were tested before switching to a new group of fish. After five fish from each group had been tested, the process was repeated for up to four cohorts for the entire experiment.

3D Markerless Pose Estimation (DeepLabCut)

Equipment: We used a computer dedicated to behavioral data acquisition and analysis that was based on a Dell Precision 3630 workstation with the following specifications: Windows 10 operating systems, Intel Xeon E-2246G processor, 64 GB RAM, multiple 2TB SSD hard drives, EVGA GFORCE RTX 2080Ti video card, dual 24” 4K monitors, Dell Thunderbolt 3 PCIe Card, OWC Mercury Elite Pro Dock (TB3RSDK24T) - 24TB Thunderbolt 3 Dock and Dual-Drive RAID configured as 12TB RAID 1.

Installation: Our GPU equipment required the installation of Tensorflow 1.12 with the NVIDIA CUDA package prior to installing multi-animal DeepLabCut2.2b8 (maDLC; [42]Mathis et al. 2018, [43]Nath et al. 2019), Python 3.6, and all dependencies in an Anaconda virtual

environment according to (https://github.com/DeepLabCut/DeepLabCut/blob/master/docs/installation.md).

Detailed tutorials for using maDLC with a single animal are available online (https://github.com/DeepLabCut/DeepLabCut/blob/master/docs/maDLC_AdvUserGuide.md, https://www.youtube.com/channel/UC2HEbWpC_1v6i9RnDMy-dfA); however, the pertinent details of our procedure are as follows.

Dataset Curation: To reduce computational load, all video files were pre-processed by down-sampling to 1000 x 1000 px then cropping out dead pixels (i.e. black spots) on the camera sensor and extraneous portions of the video by using the video editor function of maDLC.

Project Creation: A new single animal maDLC project was created and the project config.yaml file was modified to include seven unique body parts that were easily identifiable on a larval zebrafish (left_eye, right_eye, swim_bladder, tail_1 (near the base), tail_2, tail_3, tail_4 (tail tip), Fig. 1a). The skeleton was initially created by forming individual connections between the seven body parts in the config.yaml file. We then extracted 20 frames per video from a curated set of ten videos that contained representative examples of the target behaviors and experimental treatments. The seven body parts were labeled on the fish in each frame using the graphical user interface (GUI). The annotated frames were checked for accuracy and multiple additional skeletal connections between the seven body parts were added using the skeleton builder GUI pop up window, helping maDLC learn faster and create accurate models.

Pose Estimation: The training dataset was created using cropped images (400 x 400 px) to reduce computational loading and the default setting of Resnet-50 pre-trained network weights, and imgaug data augmentation. We set the display iterations to 100, save iterations to 1000, and trained the network until the all of the loss parameters plateaued at 100,000 iterations. The network was evaluated (PCK values close to 1, RMSE values low) and cross-validated using the default parameters.

664 *Identity Tracking:* Curated videos were analyzed and the detections (pickle files) were
665 assembled into tracklets (h5 files) using the box method, providing superior results for these
666 data compared to the skeleton method
667 (https://github.com/DeepLabCut/DeepLabCut/blob/master/docs/maDLC_ UserGuide.md). The
668 interactive tracklet GUI was launched and the original videos with the newly created labeled
669 body parts were used to correct for outliers in the tracklet data files. Jitter and wholesale
670 misidentification of the body part data were changed and saved.
671 *Post Processing:* The results were plotted for each video and a new labeled video was
672 created using the original curated videos and the refined tracklet data. The labeled output
673 videos were checked for labeling accuracy and there was no need to extract additional frames
674 to augment the data set. Novel videos were batch processed beginning at the video analysis
675 step and ending with the plot trajectories and label videos step. Once several videos of different
676 conditions and behavioral responses could be accurately labeled, the create labeled videos step
677 was omitted to reduce computational load, increase analysis productivity, and reduce hard drive
678 space storage requirements.

679

680 *Supervised Behavioral Annotation, Classification, & Analysis (SimBA)*
681 *Definition of Rheotaxis Behavior:* We defined positive rheotaxis as when the larvae
682 swam into the oncoming water flow at an angle of 0° ± 45° for at least 100 ms. The movement
683 component was used to distinguish active swimming behavior from passive drift in cases where
684 larvae would orient into the flow, stop swimming, and drift backward without rotating in the X-Y
685 plane.
686 *Installation:* SimBAxTF-development version 68 ([44]Nilsson et al. 2020), Python 3.6, Git,
687 FFmpeg, and all necessary dependencies were installed in a separate Anaconda virtual
688 environment: (https://github.com/sgoldenlab/simba/blob/master/docs/installation.md).

689 *Dataset Curation*: The pre-processed video files used in maDLC analysis were
690 converted to the AVI format using the video editor function of SimBA.

691 *Build Classifiers*

692 *Project Creation:* A new SimBA project was created according to Scenario 1 as shown
693 here: https://github.com/sgoldenlab/simba/blob/master/docs/Scenario1.md. Before the project
694 config file was generated, we selected the user defined pose configuration option and the DLC-
695 multi animal options. The user-defined pose configuration nomenclature must match the body
696 parts and individual animal labels used in the maDLC config file. Next, several curated videos of
697 fish from different treatments that displayed ideal examples of rheotaxis were imported into the
698 project folder. Then the h5 files (final tracklet data) generated by DLC for these videos were
699 imported. Last, the frames of each video were extracted into the project.

700 *Load Project:* The project was loaded into SimBA and the video parameters were set for
701 each of the curated videos. We made certain to set the correct frame rate (fps), resolution, and
702 pixel measurements (px/mm), as these settings affected downstream analyses. Outlier
703 correction was achieved by selecting two body parts that were reliably labeled by DLC but not
704 too close together on the animal (e.g. swim_bladder, tail_3); movement criterion was set to 0.7;
705 location criterion was set to 1.5 ([44]). Features were extracted using a custom R script, which is
706 only possible within the development version of SimBA. Rheotaxis behavior was labeled (i.e.
707 annotated were created for predictive classifiers) for each of the curated videos, but one was
708 not annotated and was set aside for validation. The model was created by training it according
709 to the default machine model settings, hyperparameters, and model evaluation settings listed in
710 Scenario 1 ([44]). Model validation was done using the aforementioned curated video, its
711 associated csv file that was previously set aside without annotation, and the model file that was
712 just created. Throughout the video, the interactive plot was used to evaluate the probability
713 threshold (i.e. the smallest peaks) where rheotaxis was accurately predicted by the model and

the minimum duration of each predicted rheotaxis event. These values became the discrimination threshold and minimum behavior bout length settings when we ran the machine model. All options were chosen during the analysis of the machine results and output files were saved in the project_folder/ logs subdirectory. Subsequent analyses were performed in R using the csv data files located in the machine_results subdirectory of the project/csv directory.

At this point the model was created and was used to predict rheotaxis on novel videos as outlined in Scenario 2: (https://github.com/sgoldenlab/simba/blob/master/docs/Scenario2.md #part-3-run-the-classifier-on-new-data). Videos and data files were archived after they were processed and analyzed to avoid reanalyzing them when new videos and data were added for analysis.

Data Analysis

Because rheotaxis data were limited to instances when fish swam at angles 0° ± 45° under flow conditions, they were compared to random swimming data of fish with a body angle of 0° ± 45° under no flow. The only exceptions to this procedure were for the angular comparisons among groups where the total data set of orientation angles was used to determine if the fish were randomly distributed under no flow (Fig. 3) or had a natural proclivity to orient toward the front of the arena, and the X-Y (2D) spatial use density plots under no flow (Fig. 6a) and flow (Fig. 6b). Time series data were quantized into 100 ms bins because it was the lowest common bin size for videos shot at 200 and 60 fps.

Data wrangling and cleaning was performed in R ([45]) with the packages tidyverse ([46]), dplyr ([47]), plyr ([48]), and readbulk ([49]). Figures and graphs were created with packages circular ([50]), ggplot2 ([51]), and viridis ([52]). The Rayleigh statistical tests (V-test) of uniformity for circular data in a specified mean direction (mu = 0°) and the Watson-Wheeler tests for differences in the grand mean body angle or angular variance (the test does not specify which parameter differs)

were performed with the package CircMLE ([53]). The mean duration, number, total distance travelled and mean latency to the onset of rheotaxis events were calculated for 10 s bins (no flow, initial and final flow) using the SimBA developer version. The generalized linear mixed models with post hoc t-tests using the Satterthwaite method were performed in R with the packages lmerTest ([54]) and lme4 ([55]), and the significance values for fixed effects were done using stats ([45]) for type III ANOVAs. The packages zoo ([56]) and spectral ([57]) were used to convert data into times series and perform spectral decomposition analyses, respectively.

Declaration of interests:

The authors declare no competing financial or non-financial interests.

Acknowledgments: We would like to thank David Lee for editorial support and Mark Warchol for feedback on the manuscript. This work was supported by the National Institute on Deafness and Other Communication Disorders R01DC016066 (L.S.), NIDA R00DA045662 (S.A.G.), NIDA P30 DA048736 (S.R.O.N. and S.A.G.), NARSAD Young Investigator Award 27082 (S.A.G.).

REFERENCES

1 Chagnaud, B. P. & Coombs, S. in *The Lateral Line System* (eds Sheryl Coombs, Horst Bleckmann, Richard R. Fay, & Arthur N. Popper) 151-194 (Springer New York, 2014).

2 Van Trump, W. J. & McHenry, M. J. The lateral line system is not necessary for rheotaxis in the Mexican blind cavefish (Astyanax fasciatus). *Integr Comp Biol* **53**, 799-809, doi:10.1093/icb/ict064 (2013).

3 Lyon, E. P. ON RHEOTROPISM. I. — RHEOTROPISM IN FISHES. *American Journal of Physiology-Legacy Content* **12**, 149-161, doi:10.1152/ajplegacy.1904.12.2.149 (1904).

4 ARNOLD, G. P. RHEOTROPISM IN FISHES. *Biological Reviews* **49**, 515-576, doi:https://doi.org/10.1111/j.1469-185X.1974.tb01173.x (1974).

5 Suli, A., Watson, G. M., Rubel, E. W. & Raible, D. W. Rheotaxis in larval zebrafish is mediated by lateral line mechanosensory hair cells. *PLoS One* **7**, e29727, doi:10.1371/journal.pone.0029727 (2012).

6 Pavlov, D. & Tyuryukov, S. The role of lateral-line organs and equilibrium in the behavior and orientation of the dace, Leuciscus leuciscus, in a turbulent flow. *JOURNAL OF ICHTHYOLOGY C/C OF VOPROSY IKHTIOLOGII* **33**, 45-45 (1993).

7 Pavlov, D. S. & Tjurjukov, S. N. Reactions of dace to linear accelerations. *Journal of Fish Biology* **46**, 768-774, doi:https://doi.org/10.1111/j.1095-8649.1995.tb01600.x (1995).

8 John C. Montgomery, C. F. B. A. G. C. The lateral line can mediate rheotaxis in fish. *Nature*, 960-963 (1997).

9 Baker, C. F. & Montgomery, J. C. Lateral line mediated rheotaxis in the Antarctic fish Pagothenia borchgrevinki. *Polar Biology* **21**, 305-309, doi:10.1007/s003000050366 (1999).

10 Baker, C. F. & Montgomery, J. C. The sensory basis of rheotaxis in the blind Mexican cave fish, Astyanax fasciatus. *Journal of Comparative Physiology A* **184**, 519-527, doi:10.1007/s003590050351 (1999).

11 Dykgraaf, S. Untersuchungen über die Funktion der Seitenorgane an Fischen. *Zeitschrift für vergleichende Physiologie* **20**, 162-214, doi:10.1007/BF00340757 (1933).

12 Bak-Coleman, J., Court, A., Paley, D. A. & Coombs, S. The spatiotemporal dynamics of rheotactic behavior depends on flow speed and available sensory information. *J Exp Biol* **216**, 4011-4024, doi:10.1242/jeb.090480 (2013).

13 Coombs, S., Bak-Coleman, J. & Montgomery, J. Rheotaxis revisited: a multi-behavioral and multisensory perspective on how fish orient to flow. *J Exp Biol* **223**, doi:10.1242/jeb.223008 (2020).

14 Coffin, A. B., Brignull, H., Raible, D. W. & Rubel, E. W. in *The Lateral Line System* (eds Sheryl Coombs, Horst Bleckmann, Richard R. Fay, & Arthur N. Popper) 313-347 (Springer New York, 2014).

15 Harris, J. A. *et al.* Neomycin-Induced Hair Cell Death and Rapid Regeneration in the Lateral Line of Zebrafish (Danio rerio). *Journal of the Association for Research in Otolaryngology* **4**, 219-234, doi:10.1007/s10162-002-3022-x (2003).

16 Ma, E. Y., Rubel, E. W. & Raible, D. W. Notch Signaling Regulates the Extent of Hair Cell Regeneration in the Zebrafish Lateral Line. *The Journal of Neuroscience* **28**, 2261-2273, doi:10.1523/jneurosci.4372-07.2008 (2008).

17 Hardy, K. *et al.* Functional development and regeneration of hair cells in the zebrafish lateral line. *J Physiol* **599**, 3913-3936, doi:10.1113/JP281522 (2021).

18 Kniss, J. S., Jiang, L. & Piotrowski, T. Insights into sensory hair cell regeneration from the zebrafish lateral line. *Current Opinion in Genetics & Development* **40**, 32-40, doi:https://doi.org/10.1016/j.gde.2016.05.012 (2016).

19 Pickett, S. B. & Raible, D. W. Water Waves to Sound Waves: Using Zebrafish to Explore Hair Cell Biology. *J Assoc Res Otolaryngol* **20**, 1-19, doi:10.1007/s10162-018-00711-1 (2019).

20 Olive, R. *et al.* Rheotaxis of Larval Zebrafish: Behavioral Study of a Multi-Sensory Process. *Front Syst Neurosci* **10**, 14, doi:10.3389/fnsys.2016.00014 (2016).

21 Olszewski, J., Haehnel, M., Taguchi, M. & Liao, J. C. Zebrafish larvae exhibit rheotaxis and can escape a continuous suction source using their lateral line. *PLoS One* **7**, e36661, doi:10.1371/journal.pone.0036661 (2012).

22 Oteiza, P., Odstrcil, I., Lauder, G., Portugues, R. & Engert, F. A novel mechanism for mechanosensory-based rheotaxis in larval zebrafish. *Nature* **547**, 445-448, doi:10.1038/nature23014 (2017).

23 Hernández, P. P., Moreno, V., Olivari, F. A. & Allende, M. L. Sub-lethal concentrations of waterborne copper are toxic to lateral line neuromasts in zebrafish (Danio rerio). *Hearing Research* **213**, 1-10, doi:https://doi.org/10.1016/j.heares.2005.10.015 (2006).

24 Linbo, T. L., Stehr, C. M., Incardona, J. P. & Scholz, N. L. Dissolved copper triggers cell death in the peripheral mechanosensory system of larval fish. *Environmental Toxicology and Chemistry* **25**, 597-603, doi:https://doi.org/10.1897/05-241R.1 (2006).

25 Olivari, F. A., Hernández, P. P. & Allende, M. L. Acute copper exposure induces oxidative stress and cell death in lateral line hair cells of zebrafish larvae. *Brain Research* **1244**, 1-12, doi:https://doi.org/10.1016/j.brainres.2008.09.050 (2008).

26 Williams, J. A. & Holder, N. Cell turnover in neuromasts of zebrafish larvae. *Hearing Research* **143**, 171-181, doi:https://doi.org/10.1016/S0378-5955(00)00039-3 (2000).

27 Coffin, A. B., Rubel, E. W. & Raible, D. W. Bax, Bcl2, and p53 differentially regulate neomycin- and gentamicin-induced hair cell death in the zebrafish lateral line. *J Assoc Res Otolaryngol* **14**, 645-659, doi:10.1007/s10162-013-0404-1 (2013).

28 Buck, L. M., Winter, M. J., Redfern, W. S. & Whitfield, T. T. Ototoxin-induced cellular damage in neuromasts disrupts lateral line function in larval zebrafish. *Hear Res* **284**, 67-81, doi:10.1016/j.heares.2011.12.001 (2012).

29 Bak-Coleman, J. & Coombs, S. Sedentary behavior as a factor in determining lateral line contributions to rheotaxis. *J Exp Biol* **217**, 2338-2347, doi:10.1242/jeb.102574 (2014).

30 Elder, J. & Coombs, S. The influence of turbulence on the sensory basis of rheotaxis. *J Comp Physiol A Neuroethol Sens Neural Behav Physiol* **201**, 667-680, doi:10.1007/s00359-015-1014-7 (2015).

31 Beck, J. C., Gilland, E., Tank, D. W. & Baker, R. Quantifying the Ontogeny of Optokinetic and Vestibuloocular Behaviors in Zebrafish, Medaka, and Goldfish. *Journal of Neurophysiology* **92**, 3546-3561, doi:10.1152/jn.00311.2004 (2004).

32 Mo, W., Chen, F., Nechiporuk, A. & Nicolson, T. Quantification of vestibular-induced eye movements in zebrafish larvae. *BMC Neurosci* **11**, 110, doi:10.1186/1471-2202-11-110 (2010).

33 Liao, J. C. The role of the lateral line and vision on body kinematics and hydrodynamic preference of rainbow trout in turbulent flow. *J Exp Biol* **209**, 4077-4090, doi:10.1242/jeb.02487 (2006).

34 Toro, C. *et al.* Dopamine Modulates the Activity of Sensory Hair Cells. *J Neurosci* **35**, 16494-16503, doi:10.1523/JNEUROSCI.1691-15.2015 (2015).

35 Zhang, Q. *et al.* Synaptically silent sensory hair cells in zebrafish are recruited after damage. *Nat Commun* **9**, 1388, doi:10.1038/s41467-018-03806-8 (2018).

36 Hernandez, P. P. *et al.* Sublethal concentrations of waterborne copper induce cellular stress and cell death in zebrafish embryos and larvae. *Biological Research* **44**, 7-15 (2011).

37 Johansen, J. L., Fulton, C. J. & Bellwood, D. R. Avoiding the flow: refuges expand the swimming potential of coral reef fishes. *Coral Reefs* **26**, 577-583, doi:10.1007/s00338-007-0217-y (2007).

38 Webb, P. W. Entrainment by river chub nocomis micropogon and smallmouth bass micropterus dolomieu on cylinders. *J Exp Biol* **201 (Pt 16)**, 2403-2412 (1998).

39 Burt de Perera, T. B. & Braithwaite, V. A. Laterality in a non-visual sensory modality--the lateral line of fish. *Curr Biol* **15**, R241-242, doi:10.1016/j.cub.2005.03.035 (2005).

40 Nusslein-Volhard, C. & Dahm, R. *Zebrafish*. (Oxford University Press, 2002).

41 Budick, S. A. & O'Malley, D. M. Locomotor repertoire of the larval zebrafish: swimming, turning and prey capture. *Journal of Experimental Biology* **203**, 2565-2579, doi:10.1242/jeb.203.17.2565 (2000).

42 Mathis, A. *et al.* DeepLabCut: markerless pose estimation of user-defined body parts with deep learning. *Nature Neuroscience* **21**, 1281-1289, doi:10.1038/s41593-018-0209-y (2018).

43 Nath, T. *et al.* Using DeepLabCut for 3D markerless pose estimation across species and behaviors. *Nature Protocols* **14**, 2152-2176, doi:10.1038/s41596-019-0176-0 (2019).

44 Nilsson, S. R. O. *et al.*, doi:10.1101/2020.04.19.049452 (2020).

45 R Core Team (2020). R: A language and environment for statistical computing. R Foundation for Statistical Computing, Vienna, Austria. URL https://www.R-project.org/.

46 Wickham et al., (2019). Welcome to the tidyverse. Journal of Open Source Software, 4(43), 1686, https://doi.org/10.21105/joss.01686

47 Wickham, H., François, R., Henry, L, and Müller, K. (2021). dplyr: A Grammar of Data Manipulation. R package version 1.0.3. https://CRAN.R-project.org/package=dplyr

48 Wickham, H. (2011). The Split-Apply-Combine Strategy for Data Analysis. Journal of Statistical Software, 40(1), 1-29. URL http://www.jstatsoft.org/v40/i01/.

49 Kieslich, P. J., and Henninger, F. (2016). Readbulk: An R package for reading and combining multiple data files. https://doi.org/10.5281/zenodo.596649

50 Agostinelli C. and Lund, U. (2017). R package 'circular': Circular Statistics (version 0.4-93). URL https://r-forge.r-project.org/projects/circular/

51 Wickham, H. ggplot2: Elegant Graphics for Data Analysis. Springer-Verlag New York, 2016.

52 Garnier, S. (2018). viridis: Default Color Maps from 'matplotlib'. R package version 0.5.1.https://CRAN.R-project.org/package=viridis

53 Fitak, R. R. and Johnsen, S. (2017). Bringing the analysis of animal orientation data full circle: model-based approaches with maximum likelihood. Journal of Experimental Biology, 220, 3878-3882. doi:10.1242/jeb.167056

54 Kuznetsova A, Brockhoff PB, Christensen RHB (2017). “lmerTest Package: Tests in Linear Mixed Effects Models.” Journal of Statistical Software_, *82*(13), 1-26. doi: 10.18637/jss.v082.i13 (URL:https://doi.org/10.18637/jss.v082.i13).

55 Bates, D., Maechler, M., Bolker, B., Walker, S. (2015). Fitting Linear Mixed-Effects Models Using lme4. Journal of Statistical Software, 67(1), 1-48. doi:10.18637/jss.v067.i01.

56 Zeileis, A. and Grothendieck, G. (2005). zoo: S3 Infrastructure for Regular and Irregular Time Series. Journal of Statistical Software, 14(6), 1-27. doi:10.18637/jss.v014.i06

57 Seilmayer, M. (2021). spectral: Common Methods of Spectral Data Analysis. R package version 2.0. https://CRAN.R-project.org/package=spectral

SUPPLEMENTARY INFORMATION

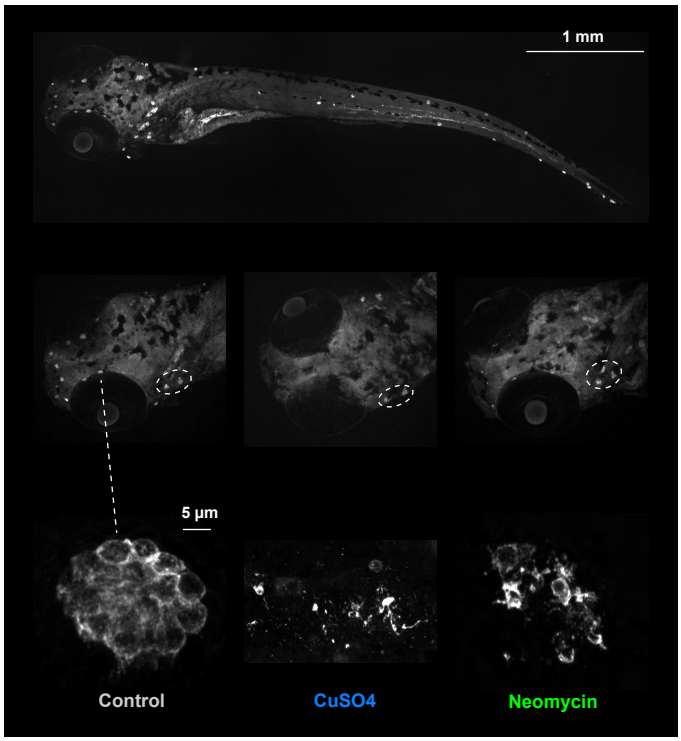

Supplementary Figure 1. Visualization of neuromast hair cell loss following $CuSO_4$ or neomycin treatment. Representative confocal images of hair cells (anti-Otoferlin immunolabel) confirmed the presence (control) or absence ($CuSO_4$, neomycin) of the sensory hair cells in the neuromasts of the lateral line in larval zebrafish. Also labeled are patches of hair cells not part of the lateral line that are within the ears and remain intact (cristae; dashed circles). Supraorbital neuromast #2 shown in detail.

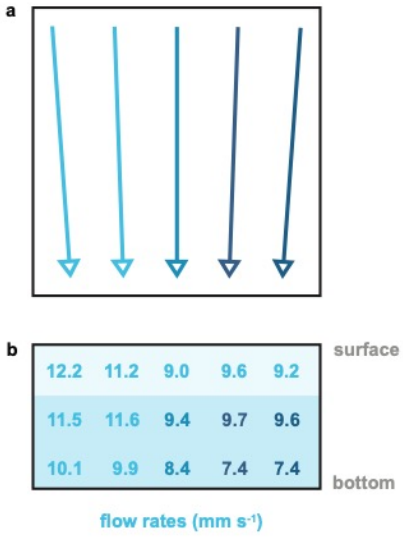

Supplementary Figure 2. Visualization of methylene blue dye tests within the experimental arena shows a laminar yet non-uniform flow field. a) The vectors are color coded according to the mean of the b) cross-sectional flow values (mm s^{-1}) from top to bottom. Each cross-sectional flow value (b) is the mean of five trials. Fish typically occupied the dark shaded area in the bottom two-thirds of the water column and very rarely swam near the surface.

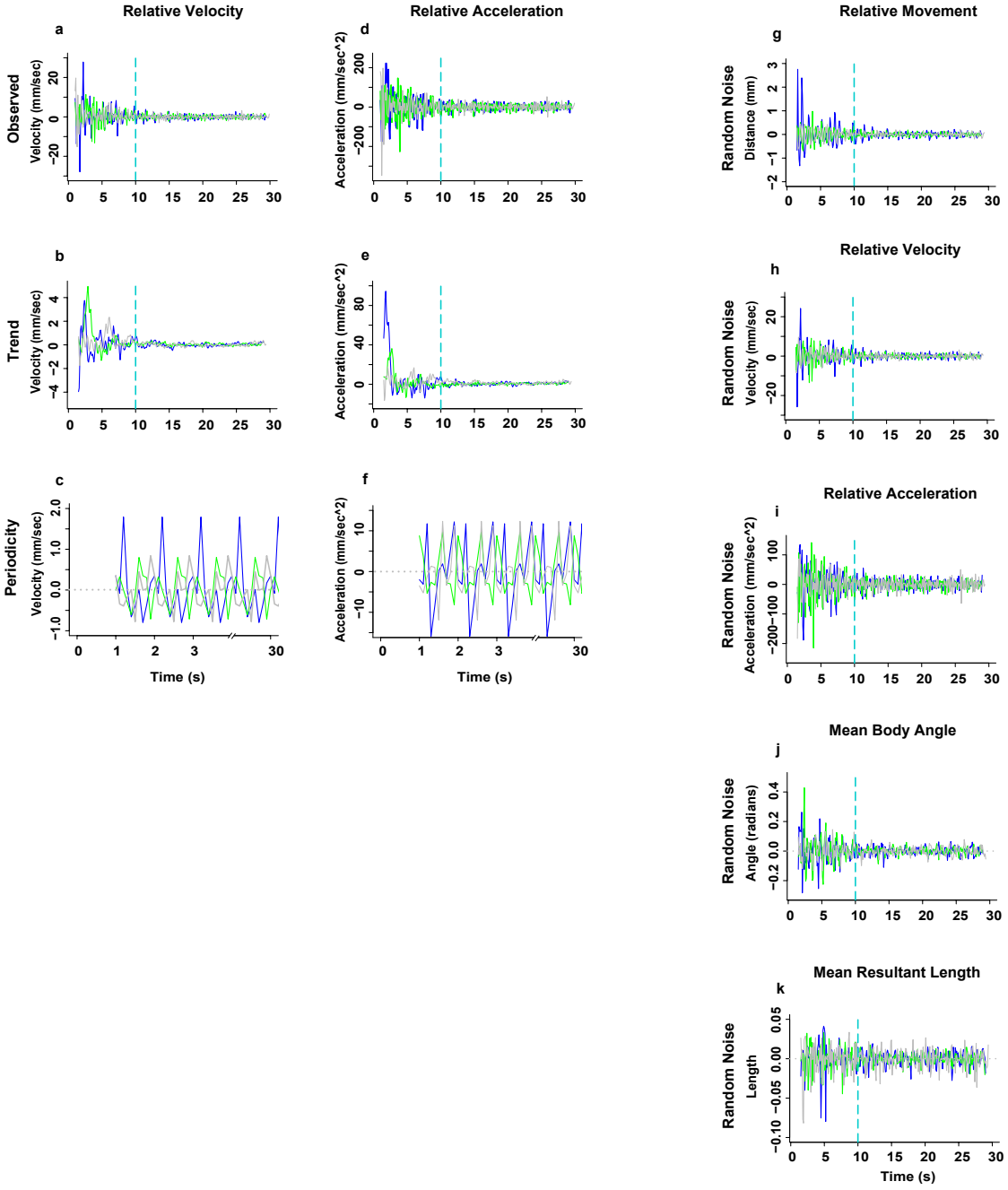

913

914 **Supplementary Figure 3. The overall trends and periodic fluctuations in the relative velocity and acceleration in rheotaxis**
915 **behavior differed among treatment groups**. Gray = control, blue = $CuSO_4$, green = neomycin. Spectral decomposition of the
916 observed data (a, d) removed the noise (h, i) to reveal the overall underlying trends (b, e) and the periodicity, or recurring
917 fluctuations (c, f) that occurred during any given 1 s of the experiment. The periodicity waveform peaks indicate the average amount
918 (amplitude), number, direction (positive = increasing; negative = decreasing), and order of occurrence for these cyclic fluctuations as
919 a function of unit time (1 s). The overall trends were that there were no differences in relative (b) velocity or (e) acceleration among
920 groups. The periodic fluctuation in relative velocity (c) and acceleration (f) was greatest in $CuSO_4$ treated fish compared to control or
921 neomycin treated fish. The noise for relative movement (g), mean body angle (j), and mean resultant length (k) are shown.

	No Flow Stimulus 1-10s *theta, rho,* ang var	Flow Stimulus 11-20s *theta, rho,* ang var	Flow Stimulus 21-30s *theta, rho,* ang var
Control	135.5° 0.084 0.916	357.9° 0.687 0.313	1.7° 0.688 0.312
CuSO4	84.8 ° 0.099 0.901	10.8° 0.530 0.470	3.1° 0.611 0.389
Neomycin	86.7° 0.090 0.900	6.1° 0.656 0.344	6.7° 0.655 0.345

Supplementary Table 1. Grand mean body angle vector parameters. *Theta* = group mean body angle; *rho* = mean length of resultant vector, where 0 = uniform distribution of individual mean body angles, 1 = perfect alignment individual mean body angles; angular variance = 1-*rho*.

	No Flow Stimulus 1-10s test stat, p-value	Flow Stimulus 11-20s test stat, p-value	Flow Stimulus 21-30s test stat, p-value
Control	-0.0595 0.9079	0.686 **< 0.001**	0.6678 **< 0.001**
CuSO4	0.009 0.4276	0.5204 **< 0.001**	0.6105 **< 0.001**
Neomycin	0.0052 0.4566	0.6522 **< 0.001**	0.6507 **< 0.001**

Supplementary Table 2. Rayleigh test of uniformity (V-test) for an expected grand mean body angle, *mu* = 0°. Among all treatments, groups under no flow were not significantly aligned to 0°, whereas groups under flow conditions were significantly aligned to 0°.

	CTL-10s p-value	CTL-20s p-value	Cu-10s p-value	Cu-20s p-value	Neo-10s p-value	Neo-20s p-value
CTL-10s test stat	-	0.4747	**2.58e-05**	0.119	**0.0357**	>0.10
CTL-20s test stat	1.49	-	**7.041e-05**	**0.0508**	0.07419	0.4502
Cu-10s test stat	21.128	19.122	-	0.04975	0.05861	**0.0090**
Cu-20s test stat	4.2573	5.9597	6.0014	-	0.311	0.1921
Neo-10s test stat	6.6655	5.2022	5.6737	2.3357	-	0.7364
Neo-20s test stat	0.1251	1.5961	9.4268	3.3000	0.61196	-

Supplementary Table 3. Watson Wheeler test for differences in either grand mean body angle or the distribution of the individual mean angles (*the test does not specify*) among treatment groups under flow conditions.

GLMM	Estimate	Std. Error	df	t value	Pr(>|t|)
Stimulus (No flow v Flow 10s)	1.14950	0.10746	1390	10.697	**< 2e-16 *****
Stimulus (No flow v Flow 20s)	1.62296	0.10746	1390	15.102	**< 2e-16 *****
Treatment (Control v $CuSO_4$)	0.05485	0.11893	2068	0.461	0.64473
Treatment (Control v Neomycin)	0.04574	0.11507	2068	0.398	0.69103
Stim*Treat (CTL-10s v $CuSO_4$-10s)	-0.34246	0.16277	1390	-2.104	**0.03556 ***
Stim*Treat (CTL-20s v $CuSO_4$-20s)	-0.45260	0.16277	1390	-2.781	**0.00550 ****
Stim*Treat (CTL-10s v Neo-10s)	-0.29562	0.15749	1390	-1.877	**0.06072 .**
Stim*Treat (CTL-20s v Neo-20s)	-0.36519	0.15749	1390	-2.319	**0.02055 ***

ANOVA (III)	Sum Sq	Mean Sq	NumDF	DenDF	F value	Pr(>F)
Stimulus	660.88	330.44	2	1390	216.7689	**< 2.2e-16 *****
Treatment	29.83	14.92	2	695	9.7842	**6.449e-05 *****
Stim*Treat	15.40	3.85	4	1390	2.5249	**0.03926 ***

Supplementary Table 4. Generalized Linear Mixed Model with Satterthwaite's method of testing for differences among treatments in the mean duration of rheotaxis events. Type III ANOVA yielded significance values for fixed effects and interactions because the LME4 package in R does not identify them in its output. Significance codes: '***' 0.001, '**' 0.01, '*' 0.05, '.' 0.1

GLMM	Estimate	Std. Error	df	t value	Pr(>|t|)
Stimulus (No flow v Flow 10s)	2.65530	0.15538	1390	17.089	**< 2e-16 *****
Stimulus (No flow v Flow 20s)	2.91667	0.15538	1390	18.771	**< 2e-16 *****
Treatment (Control v $CuSO_4$)	-0.52696	0.21170	1614	-2.489	**0.0129 ***
Treatment (Control v Neomycin)	0.46123	0.20484	1614	2.252	**0.0245 ***
Stim*Treat (CTL-10s v $CuSO_4$-10s)	-0.57687	0.23535	1390	-2.451	**0.0144 ***
Stim*Treat (CTL-20s v $CuSO_4$-20s)	0.05882	0.23535	1390	0.250	0.8027
Stim*Treat (CTL-10s v Neo-10s)	0.09687	0.22772	1390	0.425	0.6706
Stim*Treat (CTL-20s v Neo-20s)	0.05290	0.22772	1390	0.232	0.8163

ANOVA (III)	Sum Sq	Mean Sq	NumDF	DenDF	F value	Pr(>F)
Stimulus	3488.9	1744.46	2	1390	547.3568	**< 2.2e-16 *****
Treatment	167.1	83.57	2	695	26.2224	**1.049e-11 *****
Stim*Treat	40.0	9.99	4	1390	3.1356	**0.01403 ***

Supplementary Table 5. Generalized Linear Mixed Model with Satterthwaite's method of testing for differences among treatments in the mean number of rheotaxis events. Type III ANOVA yielded significance values for fixed effects and interactions because the LME4 package in R does not identify them in its output. Significance codes: '***' 0.001, '**' 0.01, '*' 0.05, '.' 0.1

GLMM	Estimate	Std. Error	df	t value	Pr(>|t|)
Stimulus (No flow v Flow 10s)	0.70177	0.16338	1721	4.295	**1.84e-05 *** **
Stimulus (No flow v Flow 20s)	0.65449	0.16338	1721	4.006	**6.44e-05 *** **
Treatment (Control v $CuSO_4$)	0.18141	0.11436	695	1.586	0.11313
Treatment (Control v Neomycin)	0.30691	0.11102	706	2.764	**0.00585 ** **

ANOVA (III)	Sum Sq	Mean Sq	NumDF	DenDF	F value	Pr(>F)
Stimulus	243.652	81.037	2	1565	38.8494	**< 2.2e-16 *** **
Treatment	8.117	3.796	2	699	3.8913	**0.02086 * **

Supplementary Table 6. Generalized Linear Mixed Model with Satterthwaite's method of testing for differences among treatments in the total distance travelled during rheotaxis events. GLMM model had no interaction between stimulus and treatment. Type III ANOVA yielded significance values for fixed effects because the LME4 package in R does not identify them in its output. Significance codes: '***' 0.001, '**' 0.01, '*' 0.05, '.' 0.1

GLMM	Estimate	Std. Error	df	t value	Pr(>|t|)
Stimulus (No flow v Flow 10s)	8.460e+00	3.333e-01	2.085e+03	25.386	**< 2e-16** ***
Stimulus (No flow v Flow 20s)	1.762e+01	3.333e-01	2.085e+03	52.882	**< 2e-16** ***
Treatment (Control v $CuSO_4$)	-1.384e+00	3.569e-01	2.085e+03	-3.877	**0.000109** ***
Treatment (Control v Neomycin)	8.802e-03	2.085e+03	2.085e+03	0.025	0.979669
Stim*Treat (CTL-10s v $CuSO_4$-10s)	.904e-01	5.048e-01	2.085e+03	0.972	0.331412
Stim*Treat (CTL-20s v $CuSO_4$-20s)	1.015e+00	5.048e-01	2.085e+03	2.011	**0.044503** *
Stim*Treat (CTL-10s v Neo-10s)	-4.100e-02	4.884e-01	2.085e+03	-0.084	0.933106
Stim*Treat (CTL-20s v Neo-20s)	8.078e-02	4.884e-01	2.085e+03	0.165	0.868645

ANOVA (III)	Sum Sq	Mean Sq	NumDF	DenDF	F value	Pr(>F)
Stimulus	112476	56238	2	2089	3834.664	**< 2.2e-16** ***
Treatment	345	173	2	2089	11.764	**8.306e-06** ***

Supplementary Table 7. Generalized Linear Mixed Model with Satterthwaite's method of testing for differences among treatments in the mean latency to the onset of first rheotaxis event. GLMM model had no interaction between stimulus and treatment. Type III ANOVA yielded significance values for fixed effects and interactions because the LME4 package in R does not identify them in its output. Significance codes: '***' 0.001, '**' 0.01, '*' 0.05, '.' 0.1

GLM	Estimate	Std. Error	t value	Pr(>|t|)
Treatment (Control v $CuSO_4$)	31.9668	4.4820	7.132	**1.21e-12** ***
Treatment (Control v Neomycin)	14.6849	4.0870	3.593	**0.000332** ***
ROI (Back v Center)	4.6943	4.7014	0.998	0.318122
ROI (Back v Front)	-6.3503	4.7014	-1.351	0.176878
ROI (Back v Left)	-13.8344	4.7014	-2.943	**0.003278** **
ROI (Back v Right)	7.7325	4.7014	-1.645	0.100126
ROI*Treat (CTL-Back v $CuSO_4$-Center)	10.2432	6.3386	1.616	0.106188
ROI*Treat (CTL-Back v Neo-Center)	733.35	5.7799	3.287	**0.001023** **
ROI*Treat (CTL-Back v $CuSO_4$-Front)	18.9995	6.3386	-4.265	**2.05e-05** ***
ROI*Treat (CTL-Back v Neo-Front)	-27.0351	5.7799	0.146	0.884161
ROI*Treat (CTL-Back v $CuSO_4$-Left)	-23.8271	6.3386	-3.759	**0.000174** ***
ROI*Treat (CTL-Back v Neo-Left)	-13.3969	5.7799	-2.318	**0.020519** *
ROI*Treat (CTL-Back v $CuSO_4$-Right)	-21.5175	6.3386	-3.395	**0.000695** ***
ROI*Treat (CTL-Back v Neo-Right)	-10.7854	5.7799	-1.866	**0.062127** .

ANOVA (III)	Sum Sq	Mean Sq	Df	F value	Pr(>F)
Treatment	172565	86283	2	49.727	**< 2.2e-16** ***
ROI	778750	194687	4	112.204	**< 2.2e-16** ***
Treatment*ROI	135133	16892	8	9.735	**1.93e-13** ***

Supplementary Table 8. Generalized Linear Model tests for differences in the two-dimensional X-Y spatial use among treatments. GLM model included fixed effects of stimulus and treatment, and the effect of the interaction between stimulus and treatment. ANOVA yielded significance values for fixed effects and interactions because the LME4 package in R does not identify them in its output. Significance codes: '***' 0.001, '**' 0.01, '*' 0.05, '.' 0.1

	Control	Control	Control	$CuSO_4$	$CuSO_4$	$CuSO_4$	Cu-Ctl	Cu-Ctl	Neomycin	Neomycin	Neomycin	Neo-Ctl	Neo-Ctl
Variable	Min	Max	Range	Min	Max	Range	ΔRange	ΔRange (factor)	Min	Max	Range	ΔRange	ΔRange (factor)
mov	-0.0431	0.0583	0.1014	-0.0724	0.1547	0.2270	0.1257	**2.2400**	-0.0414	0.0441	0.0855	-0.0158	*0.8437*
vel	-0.7762	0.8416	1.6178	-0.7991	1.7910	2.5900	0.9723	**1.6010**	-0.7129	0.7997	1.5126	-0.1051	*0.9350*
acc	-11.8950	12.3300	24.2250	-15.8962	12.1951	28.0914	3.8664	**1.1596**	-8.1738	9.7733	17.9471	-6.2779	*0.7409*
angle	-0.0158	0.0107	0.0265	-0.0087	0.0145	0.0231	-0.0034	*0.8729*	-0.0162	0.0256	0.0418	0.0153	**1.5766**
res L	-0.0052	0.0075	0.0127	-0.0038	0.0023	0.0061	-0.0066	*0.4832*	-0.0026	0.0028	0.0054	-0.0074	*0.4219*

Supplementary Table 9 (Based on Fig. 8c, g, k, o, s). Lateral line ablation by drug treatment (Cu, Neo) shifts the range in overall amplitude of linear (*mov, vel, acc*) and angular (*angle, res L*) seasonality data relative to those of the control (Ctl) group. Movement parameters in which the amplitude increased in treatment fish relative to controls are indicated in **bold**, whereas those that decreased are in *italics*.

		Control	$CuSO_4$	Cu-Ctl	Cu-Ctl	Neomycin	Neo-Ctl	Neo-Ctl	Control	$CuSO_4$	Cu-Ctl	Cu-Ctl	Neomycin	Neo-Ctl	Neo-Ctl
Variable	Dominant Peak	Freq (1/s)	Freq	ΔFreq (1/s)	Net Shift Freq 1-3	Freq	ΔFreq (1/s)	Net Shift Freq 1-3	Power	Power	ΔPower (factor)	Net Shift Pwr 1-3	Power	ΔPower (factor)	Net Shift Pwr 1-3
mov	1st	0.1567	0.1528	*-0.0039*	*down*	0.2118	*0.0551*	*down*	0.0169	0.0448	**2.6475**	**up**	0.0337	**1.9964**	**up**
mov	2nd	0.0267	0.1042	*0.0775*	-	0.0139	*-0.0128*	-	0.0101	0.0326	**3.2379**	-	0.0139	**1.3814**	-
mov	3rd	0.2533	0.0208	*-0.2325*	-	0.1632	*-0.0901*	-	0.0082	0.0287	**3.5016**	-	0.0129	**1.5777**	-
vel	1st	0.2533	0.1563	*-0.0971*	*down*	0.2118	*-0.0415*	*down*	1.8444	3.1181	**1.6906**	**up**	6.9068	**3.7447**	**up**
vel	2nd	1.8444	0.2604	*-1.5840*	-	0.4792	*-1.3652*	-	1.5272	2.5076	**1.6419**	-	1.4930	**0.9776**	-
vel	3rd	0.3100	0.2118	*-0.0982*	-	0.1632	*-0.1468*	-	0.7717	1.9820	**2.5683**	-	1.3884	**1.7991**	-
acc	1st	0.2500	0.2604	*0.0104*	*down*	0.2118	*-0.0382*	*down*	363.7884	502.2213	**1.3805**	**up**	938.4990	**2.5798**	**up**
acc	2nd	0.4800	0.3056	*-0.1744*	-	0.4410	*-0.0390*	-	244.0334	402.0855	**1.6477**	-	393.4430	**1.6123**	-
acc	3rd	0.3100	0.1458	*-0.1642*	-	0.2847	*-0.0253*	-	204.4871	304.1066	**1.4872**	-	346.3958	**1.6940**	-
angle	1st	0.0400	0.0382	**-0.0018**	**up**	0.0174	**-0.0226**	**up**	0.0029	0.0042	**1.4571**	**up**	0.0040	**1.3874**	**up**
angle	2nd	0.0700	0.1528	**0.0828**	-	0.1250	**0.0550**	-	0.0026	0.0014	**0.5371**	-	0.0028	**1.0712**	-
angle	3rd	0.1167	0.2083	**0.0917**	-	0.1944	**0.0778**	-	0.0009	0.0009	**1.0510**	-	0.0014	**1.6840**	-
res L	1st	0.0600	0.0313	*-0.0288*	*down*	0.1319	**0.0719**	**up**	0.0002	0.0002	**1.3167**	**up**	0.0001	*0.4215*	*down*
res L	2nd	0.3433	0.0625	*-0.2808*	-	0.2396	**-0.1038**	-	0.0001	0.0001	**1.7516**	-	0.0000	*0.7071*	-
res L	3rd	0.1667	0.1319	*-0.0347*	-	0.4097	**0.2431**	-	0.0001	0.0001	**1.3909**	-	0.0000	*0.6849*	-

Supplementary Table 10 (based on Fig. 9). The primary, secondary, and tertiary dominant frequencies (*Freq*) of the linear (*mov, vel, acc*) and angular (*angle, res L*) movement power spectra shift up or down (*±ΔFreq*) in each of the drug treatments (Cu, Neo) compared to the control (Ctl) group. The peak power (*Pwr*) for all dominant frequencies increases (+*ΔPwr*) in nearly all cases. Values for the net shift in frequency and power were determined by adding the values of the +/- relative shift (ΔFrequency, ΔPower) of all three dominant frequencies and generalizing the overall shift in frequency and power as "up" or "down". The trend of CuSO4 and neomycin ablation results in net downshifts in the frequency and net upshift in power of relative movement, velocity and acceleration and a net upshift in the frequency and power of the mean body angle. However, CuSO4 ablation results in a net downshift in the frequency and net upshift in power, whereas neomycin results in a net upshift in the frequency and net downshift in power. Movement parameters in which the amplitude increased in treatment fish relative to controls are indicated in **bold**, whereas those that decreased are in *italics*.

		Control	Control	$CuSO_4$	$CuSO_4$	Neomycin	Neomycin
Linear parameter reference	Angular parameter CCF	Lag: (+/-) before, after	Heading: right, left Variance: more, less	Lag: (+/-) before, after	Heading: right, left Variance: more, less	Lag: (+/-) before, after	Heading: right, left Variance: more, less
movement	body angle	before	left	**after**	**left**	*after*	*right*
movement	resultant length	before	less	**before**	**less**	*after*	*less*
velocity	body angle	simultaneous	right	*after*	*right*	**after**	**left**
velocity	resultant length	before	less	*after*	*less*	**before**	**less**
acceleration	body angle	**after**	**left**	*after*	*right*	**after**	**left**
acceleration	resultant length	**before**	**less**	*after*	*less*	**before**	**less**

Supplementary Table 11 (based on Fig. 10). The method, and perhaps mechanism, of lateral line ablation by. $CuSO_4$ and neomycin results in two distinct type of rheotaxis kinematics that are different from control fish. Each method has the opposite effect on the linear and angular movement parameters during rheotaxis and neither matches the phenotype of fish with an intact lateral line. Behavioral phenotypes in which an above average increase in the indicated linear variable was strongly correlated with a leftward heading that will occurr later and a decrease in angular variance that occurred previously are indicated in **bold**. Phenotypes in which an above average increase in the indicated linear variable was strongly correlated with a rightward heading and a decrease in angular variance that will occur later are indicated in *italics*.